Biophysical Chemistry 151 (2010) 119–138

Contents lists available at ScienceDirect

Biophysical Chemistry

journal homepage: http://www.elsevier.com/locate/biophyschem

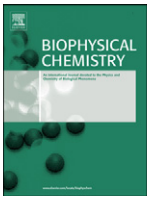

Hydrophobic hydration processes
General thermodynamic model by thermal equivalent dilution determinations

E. Fisicaro, C. Compari [*], A. Braibanti

Dept. of Pharmacological, Biological, and Applied Chemical Sciences, Physical Chemistry Section, University of Parma, Parco Area delle Scienze 27/A, I - 43124 Parma, Italy

ARTICLE INFO

Article history:
Received 10 May 2010
Received in revised form 10 June 2010
Accepted 10 June 2010
Available online 22 June 2010

Keywords:
Work enthalpy
Cavity formation
Work entropy
Cavity reduction
Thermal enthalpy
Thermal entropy

ABSTRACT

The "hydrophobic hydration processes" can be satisfactorily interpreted on the basis of a common molecular model for water, consisting of two types of clusters, namely W_I and W_{II} accompanied by free molecules W_{III}. The principle of *thermal equivalent dilution* (*TED*) is the potent tool (Ergodic Hypothesis) employed to monitor the water equilibrium and to determine the number ξ_w of water molecules W_{III} involved in each process. The hydrophobic hydration processes can be subdivided into two Classes: Class A includes those processes for which the transformation $\mathbf{A}(-\xi_w W_I \rightarrow \xi_w W_{II} + \xi_w W_{III} + \text{cavity})$ takes place with the formation of a cavity, by expulsion of ξ_w water molecules W_{III} whereas Class B includes those processes for which the opposite transformation $\mathbf{B}(-\xi_w W_{II} - \xi_w W_{III} \rightarrow \xi_w W_I - \text{cavity})$ takes place with reduction of the cavity, by condensation of ξ_w water molecules W_{III}. The number ξ_w depends on the size of the reactants and measures the extent of the change in volume of the cavity. Disaggregating the thermodynamic functions ΔH_{app} and ΔS_{app} as the functions of T (or ln$T$) and ξ_w has enabled the separation of the thermodynamic functions into *work* and *thermal* components. The work functions ΔG_{Work}, ΔH_{Work} and ΔS_{Work} only refer specifically to the hydrophobic effects of cavity formation or cavity reduction, respectively. The constant self-consistent *unitary* ($\xi_w = 1$) work functions obtained from both large and small molecules indicate that the same *unitary* reaction is taking place, independent from the reactant size. The thermal functions ΔH_{Th} and ΔS_{Th} refer exclusively to the passage of state of water W_{III}.

Essential mathematical algorithms are presented in the appendices.

1. Introduction

We have completed the thermodynamic analysis of different processes [1–4] that, at first sight, would appear to be uncorrelated, namely

(a) dissolution in water of hydrophobic gases and hydrophobic liquids,
(b) protein denaturation,
(c) micelle formation in water,
(d) hydrophobic association (so-called hydrophobic bond),
(e) protonation of carboxylato anions,
(f) complex formation between substrate and protein,
(g) effect of polar substituent on heat capacity,
(h) effect of charged substituent on the structure of the solvent.

These reactions are defined as "hydrophobic hydration processes", with a definition that is apparently self-contradictory because "hydrophobic" means that a substance shows aversion for water (literally "fearing water") and tends to escape from water (*e.g.* with low solubility) whereas hydration means that such substances, liking water tend to be hydrated. Actually both aspects are present in both processes: hate and love.

All the processes on the list are of great concern for biophysical chemists because they all take place in water, which is an essential component of every living organism. The introduction of the concepts of hydrophobic bonding [5] and hydrophobic effect [6] has occupied a large part of the literature for many decades. The hydrophobic effect consists of the preference by an apolar molecule or by the apolar tail of a molecule to reside in an apolar non-aqueous environment. This tendency was measured by Tanford [7,8] by determining the free energy change of amino-acids when dissolved in water and when in ethanol, by taking glycine as zero on the scale. The hydrophobic effect was considered entropy-driven by attributing the increase in entropy to the disordered water molecules expelled from the interface between the two apolar tails. Ben-Naim [9] speaks of hydrophobic interaction and evaluates the energy of this interaction.

The solubility of noble and apolar gases has been studied and discussed with the aim of clarifying the interaction between apolar substances and water and hence the origin of the hydrophobic effect. It was observed [10] that apolar molecules form very stable crystalline hydrates, in which a polyhedral cage of water molecules forms a cavity that hosts the apolar substance. These hydrates are relatively stable and

---

[*] Correponding author. Tel.: +39 0521 905033; fax: +39 0521 905026.
E-mail address: compari@unipr.it (C. Compari).

0301-4622/$ – see front matter © 2010 Elsevier B.V. All rights reserved.
doi:10.1016/j.bpc.2010.06.001

show large negative heats of formation with values that are nearly constant ($\Delta H = -65 \pm 4$ kJ mol^{-1}) independently of the size of the apolar molecule. This does not imply the formation of a bond between apolar moiety and water, although an interaction with the structure of the solvent certainly takes place. It is referred to as hydrophobic hydration. The negative enthalpy change could be due not to a bonding but to solvent reorganisation. Guillot and Giussani [11] evaluated the temperature dependence of hydrophobic hydration by molecular dynamic calculations of the solubility of rare gases or methane in water. They found that the evaluation of the pair distribution function between solute and solvent led to the establishing of the formation of clathrate type cages around the solute. Lee and Graziano [12] suggest the hypothesis that the transfer of a hydrophobic molecule from non-aqueous phase to water involves two different but related compensation behaviours. The hydrophobic hydration is accompanied by solvent reorganisation, which is a compensating process, and, as such, it should be irrelevant as far as the free energy of hydrophobic bond is concerned. They conclude that the true cause of the hydrophobicity must be sought elsewhere than in solvent reorganisation. Graziano [13] has studied the entropy convergence phenomenon in hydrophobic hydration.

The formation of micelles was attributed to the hydrophobic effect that brings the apolar tails of the molecules to aggregate.

The process of protein denaturation was studied from a thermodynamic point of view by Privalov [14–18], Sturtevant [19,20], Brandts [21], Lumry [22,23]. Recently, R. Lumry [22] and D. J. Winzor and C. M Jackson [24] have raised some doubts about whether the thermodynamic data can be usefully applied to isothermal processes. Lumry thinks that enthalpy, internal energy, entropy and volume data are generally suspect since they have rarely been analysed so as to take the two species of water into account and puts forward the hypothesis of a separation between work (or motive) and thermal parts of the thermodynamic functions. According to Winzor and Jackson possible side reactions should be considered. We observe, however, that the model that we are proposing actually takes into account two types of water clusters, *i.e.* W_I and W_{II}, as required by Lumry, together with free water molecules W_{III}. As far as side reactions are concerned, the side reaction that we have taken into account in micelle formation, in solubility of non-polar substances, in protonation of carboxylic acids, in bio-complex formation and in protein denaturation is the change of phase of water W_{III} that can either melt by leaving water W_I or condense into water W_I. In some of the processes the side reaction of protonation of the carboxylic sites is also considered. The terms associated with the phase transitions of water W_{III} of enthalpy and entropy functions will result to form the thermal parts of the thermodynamic functions, as suggested by Lumry, while the terms associated to the real hydrophobic reactions of cavity formation or cavity reduction constitute the work parts.

2. Water structure and thermodynamic function disaggregation

All the processes considered take place in water, and hence the assumption of a structure for liquid water is essential. The structure of liquid water (Fig. 1) is assumed to consist of three species in equilibrium:

1) water W_I consisting of clusters formed by m molecules,
2) water W_{II} consisting of clusters or short chains formed by $(m-1)$ molecules,
3) water W_{III} formed by single free water molecules.

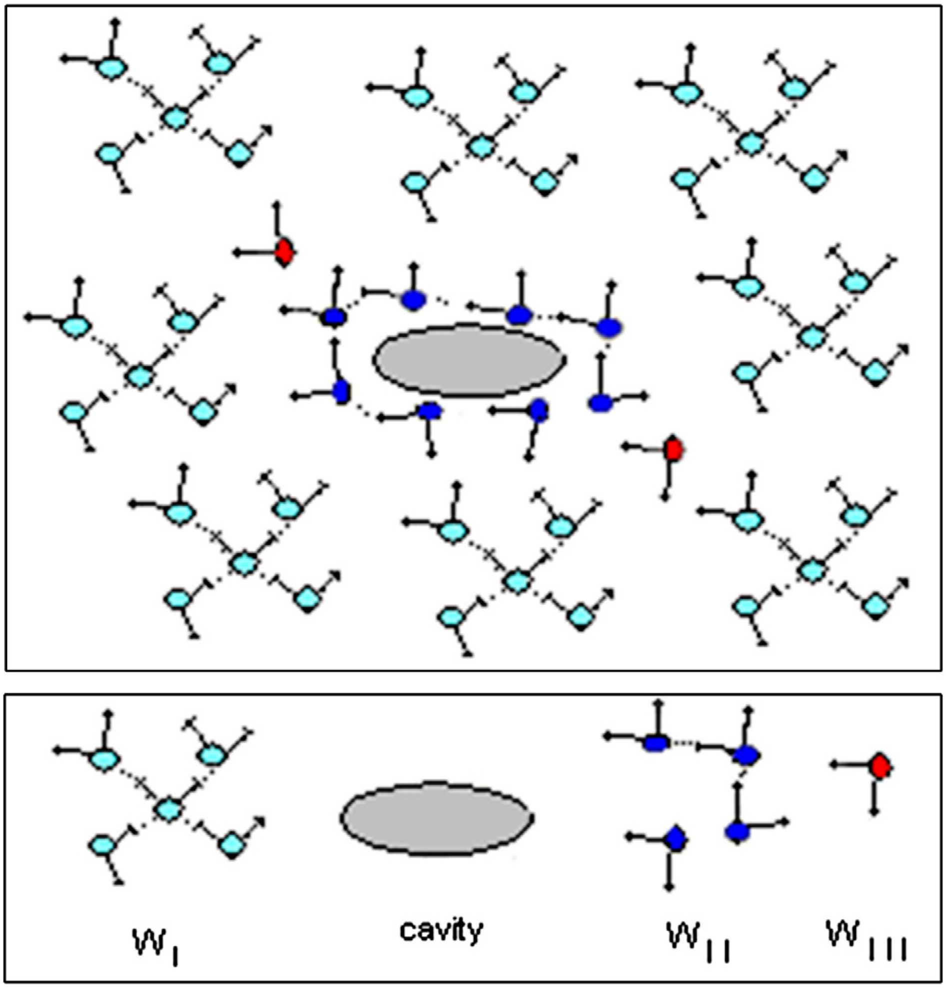

Fig. 1. Structures of water. The transformation from W_I to $(W_{II} + W_{III})$ with formation of a cavity takes place in the presence of a hydrophobic molecule.

Water W_I constitutes the bulk, water W_{II} forms sheaths around a cavity containing the solute molecule and W_{III} is moving freely in the interstices. The transformation from W_I to W_{II} with expulsion of W_{III} takes place in the presence of a hydrophobic molecule and has the effect of creating a cavity to host the solute molecule. The volume of the cavity depends on the number ξ_w of water molecules expelled. In some types of reactions, the opposite process takes place with transformation of W_{II} into W_I with condensation of molecules W_{III} and consequent filling of part of the cavity. We can, therefore, subdivide the hydrophobic hydration processes into two Classes: Class A includes those processes for which the transformation $\mathbf{A}(-\xi_w W_I \rightarrow \xi_w W_{II} + \xi_w W_{III} + \text{cavity})$ takes place with the formation of a cavity, by expulsion of ξ_w water molecules W_{III} whereas Class B includes those processes for which the opposite transformation $\mathbf{B}(-\xi_w W_{II} - \xi_w W_{III} \rightarrow \xi_w W_I - \text{cavity})$ takes place with reduction of the cavity, by condensation of ξ_w water molecules W_{III}.

The analysis of thermodynamic functions of these processes started from the study of the changes in the standard free energy with temperature. More exactly, we analysed the diagrams

$$\left(-\Delta G^{\emptyset}_{app}\right) / RT = \ln K_{app} = f(1/T). \tag{1}$$

The constant K_{app} can be either: in the processes (*a*) the solubility constant $k_{sol} = x_2$ (molar fraction), in the processes (*b*) the denaturation constant K_{den} between native and denatured state, in the processes (*c*) the micelle formation constant $K_{mic} = 1/(cmc)$, in the processes (*d*) the protonation constant K_H, in the complexation processes (*e*) the formation constant K_f, *etc.* We found that in this kind of diagram for any process examined the interpolation line was invariably a curve. Some of the diagrams show a minimum at temperatures near ambient temperature (Fig. 2), others present a maximum in the same range of temperatures (Fig. 3).

The different shapes of the curves are strictly bound to the type of equilibrium with water involved in a process, and constitute a valid criterion to subdivide the processes into the two Classes:

Class A:
  (1) dissolution in water of non-polar gases,
  (2) dissolution in water of non-polar liquids,
  (3) protein denaturation,
  (4) protonation of carboxylato anions.
Class B:
  (1) micelle formation in water,
  (2) complex formation between substrate and protein,
  (3) effect of polar substituent on heat capacity,
  (4) effect of charged substituent on solvent,
  (5) hydrophobic association (so-called hydrophobic bond).

The importance of the type of curvature that characterises the processes derives from the fact that both types of curve have a well-defined kind of tangent (see Appendix A). In fact, the tangent to the function of Eq. (1) is calculated by the van't Hoff equation

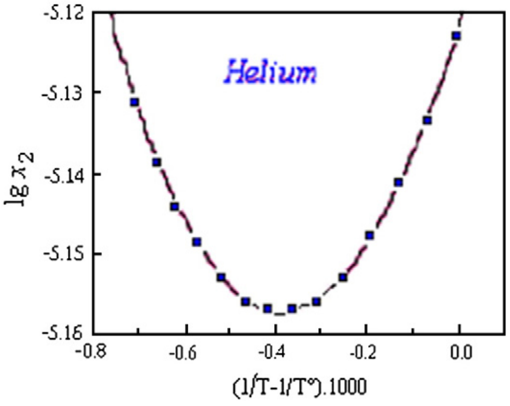

Fig. 2. Solubility of helium as the function of reciprocal temperature.

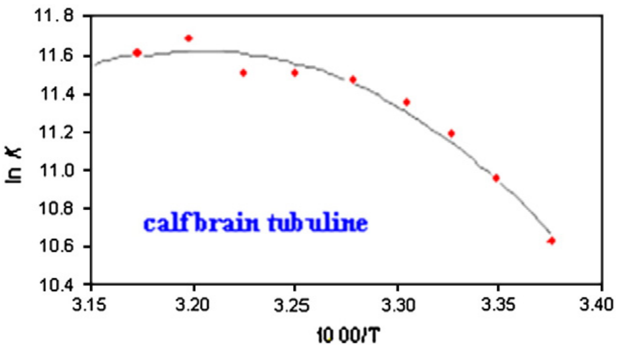

Fig. 3. Bio-complex constant as the function of reciprocal temperature.

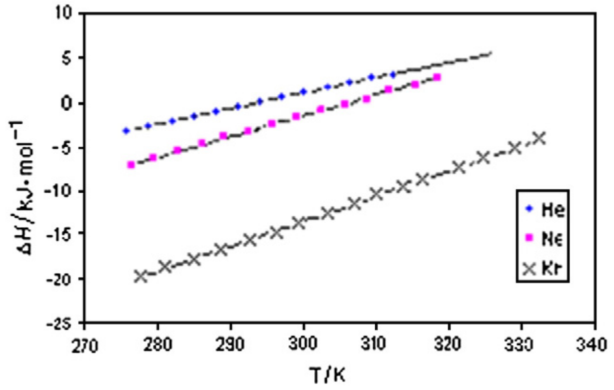

Fig. 4. Plot of ΔH_{app} against *T*/K for noble gases. The slope depends on gas radius.

$$\partial(\ln K_{app}) / \partial(1/T) = -\Delta H_{app} / R \tag{2}$$

It is clear that the two types of curves have tangents with opposite slopes and hence opposite trends of the enthalpy. In any process of Class A, the reaction is apparently exothermal at low temperature (cf. right hand branch of the curve in Fig. 2) and, passing through an adiabatic point at the minimum of the curve, it becomes endo-thermal at higher temperatures. In contrast, in any process of Class B, the reaction is apparently endo-thermal at low temperature (cf. right hand branch of the curve in Fig. 3) and, passing through an adiabatic point at the maximum of the curve, it becomes exothermal at higher temperatures. By calculating this derivative at any temperature of the interval and by plotting ΔH_{app} against *T*, we obtain, for every reaction considered, an expression

$$\Delta H_{app} = \Delta H_{Work} + \Delta C_p T = \Delta H_{Work} + \Delta H_{Th} \tag{3}$$

with slope $\Delta C_p > 0$ for Class A (Fig. 4) and $\Delta C_p < 0$ for Class B (see Glossary).[1]

If we, for each process and each temperature, calculate ΔS_{app} by means of the Helmholtz–Gibbs equation

$$T\Delta S_{app} = \Delta H_{app} - \Delta G_{app} \tag{4}$$

and then plot this entropy function against ln*T*, we obtain a linear expression (Fig. 5)

$$\Delta S_{app} = \Delta S_{Work} + \Delta C_p \ln T = \Delta S_{Work} + \Delta S_{Th} \tag{5}$$

---

[1] The reader can refer to the Glossary at the end of this paper to check meaning of symbols and subscritps.

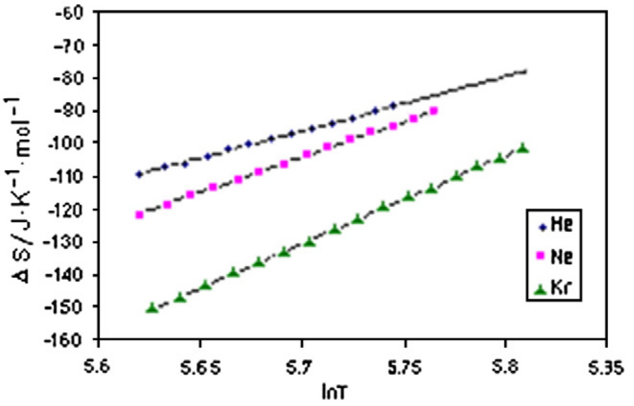

Fig. 5. Plot of ΔS_{app} against ln$T$ for noble gases. The slopes are the same as those of Fig. 4.

where the slope ΔC_p is exactly the same as that obtained from Eq. (3) for the enthalpy of that compound. The linearity of the plots $\Delta H = f(T)$ and $\Delta S = f(\ln T)$ and the coincidence of the slopes ΔC_p for the same substance follow from precise properties of mathematical functions [4].

A high value of ΔC_p has been recognised as typical of every hydrophobic hydration process. It contains significant information relative to the process: (*i*) the 'sign' of ΔC_p is indicative of the Class (A or B) each process belongs to and of the type ($+\Delta V$ or $-\Delta V$) of change in volume of the cavity, and (*ii*) the 'magnitude' of ΔC_p is proportional to the molecular size of the reactant and to the extent of change in volume of the correspondent cavity. In fact, the change in volume of the cavity depends on the stoichiometric number ξ_w of water molecules W_{III} changing phase in each process and creating or reducing the cavity.

It is thus possible, as shown in Eqs. (3) and (5) disaggregate the experimental functions ΔH_{app} and ΔS_{app} into two parts, each of which refers to a particular section of the process: the *thermal* components ΔH_{Th} and ΔS_{Th} refer to the change of phase of water W_{III}, whereas the enthalpy function, extrapolated to $T = 0$, ΔH_{Work} and the entropy function, extrapolated to ln $T = 0$, ΔS_{Work} constitute the *work* components. The work functions represent the parts of the thermodynamic functions referred to the real molecular work of cavity formation (in Class A) or cavity reduction (in Class B) and coupled reactions. They are devoid of thermal energy and, therefore, independent from the temperature. They can be, on their turn, disaggregated in different steps, as shown in Appendix C.

3. Thermal equivalent dilution and stoichiometric coefficient of water W_{III}

We can now analyse the origin of the slopes ΔC_p in Eqs. (3) and (5) and their molecular implications. The meaning of the slopes ΔC_p can be understood by recalling the principle [25] of *thermal equivalent dilution* (*TED*, see Appendix B), which is a corner stone in the study of hydrophobic hydration.

The *TED* method based on the assumption of the validity of the so-called "Ergodic Hypothesis" [26] appears as a potent experimental tool to evaluate the variation of the equilibrium constants with the temperature in every hydrophobic hydration process. It has been applied by us [27] starting from the study of the protonation of carboxylic acids. By applying the Eq. (A.4) to the analysis of the plots of Eq. (1), we have been able to evaluate the number n_w of water molecules W_{III} involved in each reaction. This has been achieved by measuring the variation of virtual dilution $(-n_w \partial \ln[(W_{III})_T] / \partial \ln T \neq 0)$, and hence of equilibrium constant, brought about by the water molecules W_{III} when the temperature is changing. If we indicate as $[(W_{III})_T]$ the activity of W_{III}, we can verify that the variation of the virtual dilution $dW_{III} = 1/[(W_{III})_T]$ is the unique cause of the curvature in the plots of Fig. 2, with a minimum, and in Fig. 3, with a maximum (we remind that, in contrast, if there were no virtual dilution $(-\partial \ln[(W_{III})_T] / \partial \ln T = 0)$ the plot of the function in Eq. (1) should give a straight line as any normal van't Hoff plot). In fact, the curvature with a minimum depends exclusively on the slope $\Delta C_p > 0$ of Eqs. (3) and (5) and the curvature with a maximum depends on the slope $\Delta C_p < 0$ of Eqs. (3) and (5). This means that the curvatures depend on the number n_w which is the power of the activity $[(W_{III})_T]$. In fact, by applying *TED*, the slope ΔC_p can be deconvoluted, as a product of two factors (see Appendix A, Eq. (A.9))

$$\Delta C_p = C_{p,w} n_w \tag{6}$$

where $C_{p,w} = 75.36\ \mathrm{J\,K^{-1}\,mol^{-1}}$ is the isobaric heat capacity of liquid water and n_w is a number obtained by dividing the experimental ΔC_p by $C_{p,w}$. It is evident that, in the processes of Class B, the number n_w is negative.

The number n_w was assumed at first as being simply proportional to the volume of the solute and dependent upon a generic concentration of water molecules W. In the course of the subsequent researches, however, it has been proved to correspond to the real number $\xi_w = |n_w|$ of water molecules W_{III} involved in each reaction and as such we can consider it. This has open the way to determine the real number ξ_w whereby these water molecules W_{III} enter in every hydrophobic hydration process. The absolute value ξ_w was adopted because in Class B n_w is negative and the introduction of the absolute value transfers any change of sign to the associated thermodynamic quantity, with meaningful thermodynamic and molecular implications.

Being curvature and number $\xi_w = |n_w|$ necessarily connected each other, we have to conclude that the shape of the curve constitutes a valid criterion to subdivide the hydrophobic processes into two Classes, Class A with $\Delta C_p > 0$ and $\xi_w = n_w > 0$, with a minimum, and Class B with $\Delta C_p < 0$ and $-\xi_w = n_w < 0$, with a maximum. Within each Class, the amplitude of curvature, depending on the value of ξ_w is a valid parameter to distinguish the stoichiometry of each process. In fact, as shown by Eq. (A.8) for Class A and Eq. (A.10) for Class B, the slope of the function $\Delta H_{app,} = f(T)$ is a function of the number ξ_w. At the same time, as shown in Eq. (A.20), the slope of the function $\Delta S_{app} = f(\ln T)$ is exactly equal to that of enthalpy. This demonstrates the existence of one more condition necessarily valid for these relationships: the constancy of ΔC_p at different temperatures cannot be considered anymore as an assumption or an approximation, as erroneously asserted by some authors, but it is a necessary condition derived from the molecular model, because it depends only upon the stoichiometric number $\pm\xi_w$ that is constant for each reaction and does not change with the temperature as far as the stoichiometry of the reaction remains the same.

The number ξ_w is the real stoichiometric coefficient of water W_{III} involved in that specific reaction. The real meaning of ξ_w can be confirmed, for instance, by the fact that ξ_w is strictly proportional to the radius of the noble gases [2]. Moreover, by plotting the partial molar volume V_2 of alkyl compounds in their liquid state against ξ_w ($V_2 = -27.7 + 19.9\,\xi_w$), we can calculate the change of partial volume per water molecule W_{III} involved, that is $\Delta V_2 = 19.9\ \mathrm{cm^3\,mol^{-1}}\,\xi_w^{-1}$ which is very close to the value $V_2 = 18.5\ \mathrm{cm^3\,mol^{-1}}$ given by Kharakoz [27,28] for partial volume of liquid water. By considering that the relationship of the partial volume of alkyl compounds to the solution is accompanied by a general contraction of $-27.7\ \mathrm{cm^3\,mol^{-1}}$, we can conclude that a volume shrinkage takes place when the solute is added to water and as a consequence the cavity formed in the solvent to host the solute is smaller than the sum of the volumes of ξ_w molecules W_{III} expelled. This contraction of the cavity could be a consequence of the contemporary transformation of the water molecules of the cage surrounding the cavity from W_I to W_{II}. In fact, water W_{II} is attributed a higher density and hence a smaller volume than W_I.

Even the sign in $\pm\xi_w$ is thermodynamically and chemically meaningful. In the processes of Class A, where $\Delta C_p > 0$ and hence

$n_w > 0 = +\xi_w$, the positive sign indicates that a 'dissociation' reaction by ξ_w molecules W_{III} is taking place (cf. Eq. (A.1.bis)) whereas in the processes of Class B where $\Delta C_p < 0$ and hence $n_w < 0 = -\xi_w$, the minus sign indicates that an 'association' reaction by $-\xi_w$ molecules W_{III} is taking place (cf. Eq. (A.2.bis)).

These coherent responses from so many systems tell us that the *TED* principle is working, when applied to the hydrophobic hydration processes at different temperatures. It gives so reliable information for the determinations of the stoichiometric coefficient ξ_w, that it can be assumed as an experimental proof of the validity of the "Ergodic Hypothesis" itself, on which *TED* is actually based.

4. General thermodynamic scheme for Class A and Class B

One more point in favour of the real meaning of ξ_w as related to the volume of the cavity is deduced by the fact that this number enters also in the terms of the thermodynamic functions independent from the temperature, *i.e.* in the *work* functions ΔH_{Work} of Eq. (3) and ΔS_{Work} of Eq. (5). Everyone of these extrapolated values is a thermodynamic function devoid of thermal energy. The inherent relationships are developed in detail in Appendix C.

As a result of the disaggregation of the thermodynamic functions in different components, we can represent any thermodynamic function experimentally determined ΔH_{app} and ΔS_{app} as the sum of three terms, in any process of any Class. Each term is associated to a specific reaction step.

The apparent enthalpy in Class A is represented by

$$\Delta H_{app} = \Delta H_0^{(\xi_w = 0)} + \xi_w \Delta h_{for} + \xi_w C_{p,w} T \tag{7}$$

and the apparent entropy in Class A by

$$\Delta S_{app} = \Delta S_0^{(\xi_w = 0)} + \xi_w \Delta s_{for} + \xi_w C_{p,w} \ln T. \tag{8}$$

The unique general scheme of three terms is exactly reproduced for both enthalpy and entropy.

For the processes of Class B, we can find, both for enthalpy and entropy similar relationships based on three terms, and the general equations can be written

$$\Delta H_{app} = \Delta H_0^{(\xi_w = 0)} + \xi_w \Delta h_{red} – \xi_w C_{p,w} T \tag{9}$$

and

$$\Delta S_{app} = \Delta S_0^{(\xi_w = 0)} + \xi_w \Delta s_{red} – \xi_w C_{p,w} \ln T \tag{10}$$

where the minus sign in the last terms depends on the condensation reaction by $-\xi_w$ molecules W_{III}.

If we analyse in detail, as it will be shown in the following paragraphs, this general scheme, when applied to the experimental values of each series in both Classes, shows very strict and self-consistent connections. The thermodynamic scheme based on three terms has a very highly potent predictive power and is capable to explain coherently all the reactions that can be classified as hydrophobic hydration processes. Each term will be found to correspond to a specific step of a reaction.

To give an example of the general character and high predictive power of these relationships, we consider those terms that are common to all members of each Class (unitary quantities *i.e.* referred to $\xi_w = 1$), as Δh_{for} and Δs_{for} in Class A or Δh_{red} and Δs_{red} in Class B. They are referred to the processes of cavity formation in Class A or cavity reduction in Class B. It is possible to calculate from all the experimental values of Class A, a mean value $<\Delta h_{for}> = -22.2 \pm 0.7$ kJ mol$^{-1}\xi_w^{-1}$ for enthalpy and a mean value $<\Delta s_{for}> = -445 \pm 3$ J K^{-1}mol$^{-1}\xi_w^{-1}$ for entropy. This means that, by considering the very small variability ($\pm\sigma$), all the processes of Class A can be correctly considered as belonging to the same homogeneous group of reactions. In Class B, we obtain the mean value $<\Delta h_{red}> = +23.7 \pm 0.6$ kJ mol$^{-1}\xi_w^{-1}$ for enthalpy and a mean value $<\Delta s_{red}> = +432 \pm 4$ J K^{-1}mol$^{-1}\xi_w^{-1}$ for entropy, thus indicating that also the processes of Class B belong to a unique group of reactions. Moreover, if we compare each mean value of Class A with the correspondent mean value of Class B, we observe that the numerical values are almost equal and the signs only are reversed, thus strongly supporting the point of view that both in Class A and in Class B we are dealing with the same process, direct in Class A as in reaction **A**$(-\xi_w W_I \rightarrow \xi_w W_{II} + \xi_w W_{III} + \text{cavity})$ and reversed in Class B as in reaction **B**$(-\xi_w W_{II} - \xi_w W_{III} \rightarrow \xi_w W_I - \text{cavity})$.

5. Work and thermal components of thermodynamic functions

Eqs. (7)–(10) are suited to show how the distinction between non-thermal motive (or work) component and thermal kinetic (or compensation) component for both enthalpy and entropy proposed by Lumry [22,23] is applicable to every hydrophobic hydration process of both Classes.

The thermal components of enthalpy and entropy are produced in the shell of water surrounding the hydrophobic moiety, that is to say that the thermal part is produced by molecules W_{III} expelled from the sheath of water W_{II} surrounding the solute in Class A or by molecules W_{III} restructured in the bulk, by combining with W_{II} in Class B.

In Eq. (7), the first two terms of the right hand side

$$\Delta H_0^{(\xi_w = 0)} + \xi_w \Delta h_{for} = \Delta H_{Work} \tag{11}$$

compose the work heat, whereas the third term

$$\xi_w C_{p,w} T = \Delta H_{Th} \tag{12}$$

is the thermal heat. The non-thermal work (or motive) heat ΔH_{Work} (*i.e.* extrapolated to $T = 0$) is composed of the solute–solvent interaction enthalpy ($\Delta H_0^{(\xi_w = 0)}$) and of the enthalpy change ($\Delta H_{for} = +\xi_w \ \Delta h_{for}$) for cavity formation with rearrangement of water molecules from clusters W_I to clusters W_{II}. On the other hand, the thermal enthalpy ΔH_{Th} represents the kinetic energy gained by another part of the system that is ξ_w free water molecules W_{III} that change aggregation state.

Analogously for the entropy, the distinction between work and thermal components follows the same lines as for enthalpy. The first and second terms contribute to the work entropy ΔS_{Work}

$$\Delta S_0^{(\xi_w = 0)} + \xi_w \Delta s_{for} = \Delta S_{Work} \tag{13}$$

that is the entropy extrapolated to $\ln T = 0$. The first term, $\Delta S_0^{(\xi_w = 0)}$, indicates the entropy change at the solute–solvent interface and the second one, $\xi_w \ \Delta s_{for} = \Delta S_{for}$, indicates the entropy change (negative) associated with the formation of the cavity in Class A. The negative entropy for cavity formation is particularly large, and corresponds to the extension of the cavity and hence to the contraction of volume of the solvent, requiring high expenditure of entropy. Lastly, the term

$$\Delta S_{Th} = \xi_w C_{p,w} \ln T \tag{14}$$

indicates in Class A the thermal entropy, *i.e.* the entropy absorbed as heat by ξ_w water molecules W_{III} when they leave the structured bulk and start moving freely in the interstices. The relation between thermal enthalpy divided by T and thermal entropy is the same as that existing between heat of fusion divided by T and the entropy change of the melted phase.

On the whole, being $\Delta H_{Th} - T\Delta S_{Th} = 0$, we can ignore the thermal portions of enthalpy and entropy, and calculate a work free energy, by

$$\Delta G_{Work} = \Delta H_{Work} - T\Delta S_{Work} = \left(\Delta H_0^{(\xi_w = 0)} + \Delta H_{for}\right) - T\left(\Delta S_0^{(\xi_w = 0)} + \Delta S_{for}\right). \qquad (15)$$

If we analyse the composition of the work free energy ΔG_{Work} as separated from the thermal components (Fig. 6), we can appreciate the overwhelming prominence of the work entropy term $(-T\Delta S_{Work})$ in determining the unfavourable positive free energy value. It is worth noting that ΔG_{Work}, ΔH_{Work}, and ΔS_{Work} are specific thermodynamic functions of the real hydrophobic process of cavity formation in Class A, independent from the temperature. This explains the very low 'hydrophobic' solubility of non-polar gases and liquids. On the other hand, ΔH_{Th}, and ΔS_{Th} refer exclusively to the thermal energy gained in Class A by ξ_w water molecules W_{III}.

For Class B also, we can calculate the work free energy $\Delta G_{Work} < 0$ of complex formation by

$$\Delta G_{Work} = \Delta H_{Work} - T\Delta S_{Work} = (\Delta H_0^{(\xi_w = 0)} + \Delta H_{red}) - T(\Delta S_0^{(\xi_w = 0)} + \Delta S_{red}) \qquad (16)$$

where the term $-T\Delta S_{Work} < 0$, with high entropy gain ($\Delta S_{red} = +436.2 \cdot \xi_w \text{J K}^{-1} \text{mol}^{-1}$) from cavity reduction, is the main contributor to the affinity of the association (Fig. 7). The processes of Class B, we remind that hydrophobic bond is an important member of this Class, clearly result to be thermodynamically stable because, they are entropy-driven. In Class B again, the work functions ΔG_{Work}, ΔH_{Work}, and ΔS_{Work} in Eq. (16) are the true thermodynamic functions of cavity reduction and are independent from the temperature. In regard to hydrophobic bonding, we want to underline the fact that the entropy gain in hydrophobic bonding was attributed in the past not to cavity reduction rather to hypothetical dispersed water molecules supposed to be expelled from the interface between the two hydrophobic moieties. This mechanism would be not compatible with the present model.

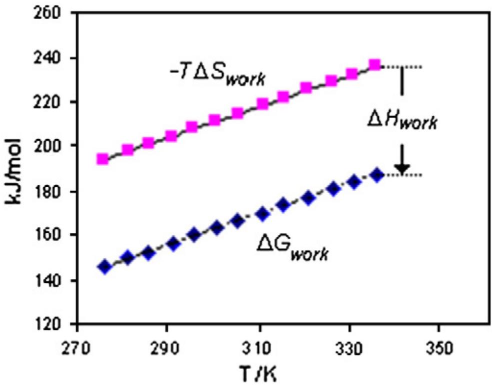

Fig. 6. Class A: components of ΔG_{Work} separated from the thermal contributions for Helium.

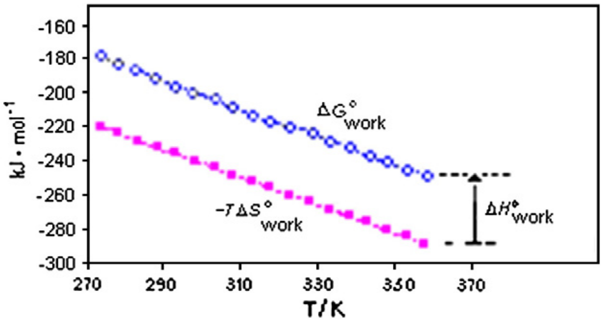

Fig. 7. Class B: the main contribution to negative free energy in micelle formation is given by the entropy term due to filling of the excess cavity. Enthalpy change is $\Delta H_{Work} = +39.9$ kJ mol^{-1}.

The thermal components ΔH_{Th}, and ΔS_{Th} refer exclusively in Class B to the thermal energy lost by ξ_w water molecules W_{III}. An interesting point to be recalled is that the thermal components ΔH_{Th} and $-T\Delta S_{Th}$ compensate each other in both Classes at any temperature and do not contribute to free energy ($\Delta G_{Th} = 0$), thus confirming the hypothesis of Lee and Graziano [12]. On the other hand, ΔH_{Th} and ΔS_{Th} separately, sum up with the corresponding work function to give ΔH_{app} and ΔS_{app}, respectively, thus affecting significantly the dependence of ΔG_{app} upon the temperature and simulating an inexistent dependence of hydrophobicity upon the temperature. The substantial distinction, however, between work and thermal functions has been ignored so far in every molecular calculation of the hydrophobic effects, thus searching for a dependence of hydrophobicity from the temperature, dependence that does not exist for ΔG_{Work}, ΔH_{Work} and ΔS_{Work} in either Class A or B.

6. Validation of the model: Class A

We can now present the molecular transformations that explain the different processes in Class A and the peculiarities of each of them. We will show how each step of the molecular mechanism conforms to a separate term of the general thermodynamic scheme. We must recall here that the processes of Class A are characterised by (*i*) a curve $\ln K_{app} = f(1/T)$ with a minimum, (*ii*) a function enthalpy vs. T represented by a straight line with positive slope, (*iii*) a function entropy vs. $\ln T$ represented by a straight line with the same positive slope as the enthalpy, and (*iv*) a number n_w (cf. Eq. (6)) that is positive and therefore according to Eq. (A.1.bis) (see Appendix A) implying a dissociation of ξ_w water molecules W_{III}.

6.1. Dissolution of non-polar gases

With reference to the solubilisation in water of non-polar substances, specifically to gases [29,30], we can look at Fig. 8. On the left of the diagram, the free molecules of non-polar gas are represented and on the right the structure of the solution is drawn with the molecule of gas imbedded in the cage in the solution. The transformation of some of the molecules W_I to W_{II} that has taken place is associated with the creation of a cavity with expulsion of ξ_w molecules W_{III}. The solute molecule is allocated in that cavity surrounded by a sheath of water W_{II}. The process can be presumed to develop through successive steps. At first, we can take it that there is only a contact between gas and water W_I without the formation of cavity. This step can be described by a contact reaction with the formation of a contact complex

$$(Kr)_{gas} + \xi_w W_I \rightarrow Kr(W_I)_{\xi_w} \qquad (17)$$

that corresponds in the enthalpy thermodynamic plane to an enthalpy change of $\Delta H_0{}^{(\xi_w = 0)} = -17.7$ kJ mol^{-1} (cf. the first term on the right hand side of Eq. (7)). In the entropy thermodynamic plane, this step corresponds to $\Delta S_0{}^{(\xi_w = 0)} = -86.4$ J K^{-1} mol^{-1}, a value which is exactly equal to the entropy change $\Delta S_{condens} = -86.9 \pm 1.4$ J K^{-1} mol^{-1} given by the Trouton constant [31] referring to the passage from vapour to liquid. We recall here that the Trouton constant has been calculated for many liquids by dividing the evaporation heat by the boiling temperature T_{eb}/K. The ratio $-\Delta H/T_{eb}$ is an entropy change. The coincidence between our result, that is referred to a process independent from the temperature (*i.e.* extrapolated to $\ln T = 0$) and independent from the cavity (*i.e.* extrapolated

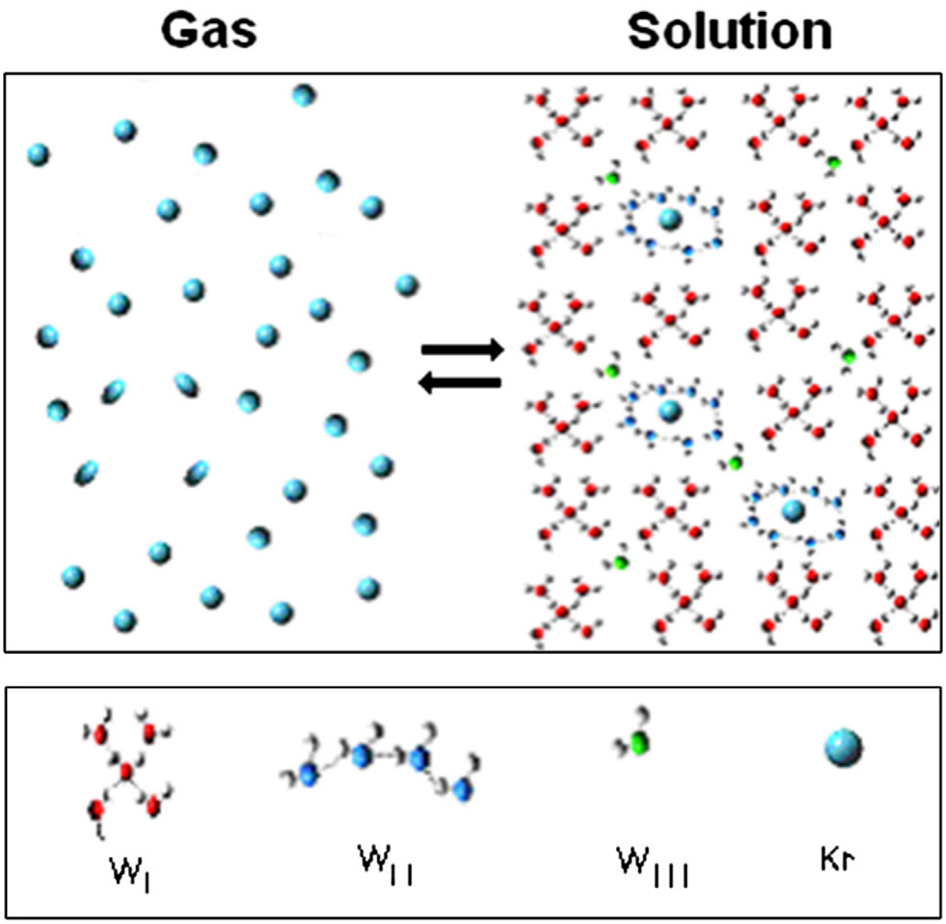

Fig. 8. Equilibrium between gas and its solution in water.

to $\xi_w = 0$), and the Trouton constant is not just a chance one, since the change of state of the molecules from gas to liquid cage is actually the same as that from vapour to liquid. The difference is that $\Delta S_{\mathrm{condens}}$ constant indicates a change of velocity of the molecules per degree whereas $\Delta S_0^{(\xi_w = 0)}$ indicates a change of dilution (cf. Ergodic Hypothesis).

The subsequent step consists of the transformation of the contact complex $\mathrm{Kr(W_I)_\xi}$ into the cage $\mathrm{Kr(W_{II})_\xi}$ with the transformation from water $\mathrm{W_I}$ to water $\mathrm{W_{II}}$ and creation of the cavity with expulsion of ξ_w water molecules $\mathrm{W_{III}}$:

$$Kr(W_{\mathrm{I}})_{\xi_w} \rightarrow Kr(W_{\mathrm{II}})_{\xi_w} + \xi_w W_{\mathrm{III}}. \tag{18}$$

By referring only to water molecules, this reaction can be alternatively written as

$$\xi_w W_{\mathrm{I}} \rightarrow \xi_w W_{\mathrm{II}} + \xi_w W_{\mathrm{III}} + cavity. \tag{19}$$

This process implies an enthalpy change $\Delta H_{for} = \Delta h_{for} \cdot \xi_w < 0$ with $\Delta h_{for} = -21.6\ \mathrm{kJ\ mol^{-1}}\,\xi_w^{-1}$ (cf. the second term on the right hand side of Eq. (7)) measuring the relative stabilisation energy of the two types ($\mathrm{W_I} \rightarrow \mathrm{W_{II}}$) of clusters surrounding the solute molecule. This stabilisation energy is proportional by way of ξ_w to the size of the cavity, perhaps, implying closer Kr–water contacts, to its surface. The unitary enthalpy change for cavity formation could be related to the observation that the crystal hydrates of apolar substances show large negative heats of formation [10] that amount to $\Delta H = -65 \pm 4\ \mathrm{kJ\ mol^{-1}}$. This value should correspond to a cavity volume equivalent to $\xi_w = -65/-21.6 \approx 3$ water molecules, that is, the average number of water molecules found by us in the solubility of noble gases.

The entropy change of this step is $\Delta S_{for} = +\xi_w\ \Delta s_{for} < 0$ (cf. the second term in the right hand side of Eq. (8)). The unitary quantity $\Delta s_{for} = -445\ \mathrm{J\ K^{-1}\ mol^{-1}}\,\xi_w^{-1}$ indicates the very large loss of entropy bound to the formation of one cavity unit (*i.e.* for $\xi_w = 1$). This term will be crucial in determining the entropy-opposed type of this reaction.

The subsequent step consists of the movement of ξ_w water molecules $\mathrm{W_{III}}$ which begin moving freely in the interstices of the structure. Associated with this step, there is the term $\xi_w C_{p,w} T$ (cf. the third term on the right hand side of Eq. (7)) corresponding to the heat absorbed by these ξ_w $\mathrm{W_{III}}$ molecules released from the cavity. This energy is necessary for free water molecules $\mathrm{W_{III}}$ to acquire the thermal energy appropriate to the temperature *T*. And in fact, the term $\xi_w C_{p,w} \ln T$ in Eq. (8) indicates the corresponding thermal entropy gained by these ξ_w molecules $\mathrm{W_{III}}$.

The total process can be represented by the reaction

$$(Kr)_{\mathrm{gas}} + \xi_w W_{\mathrm{I}} \rightarrow \left(Kr(W_{\mathrm{II}})_{\xi_w}\right) + \xi_w W_{\mathrm{III}} \tag{20}$$

where $(\mathrm{Kr(W_{II})}_{\xi w})$ represents a complex formed by the gas molecule fixed in the cage of water $\mathrm{W_{II}}$. The total reaction corresponds to the total enthalpy ΔH_{app}, which is positive above the temperature corresponding to the minimum and negative below that temperature. The exo- or endo-thermal character depends on the temperature of the experiment. This point is important because this means that we cannot infer from the response of the calorimeter if the reaction is enthalpy-driven or not.

6.2. Dissolution of non-polar liquids

The analysis of the enthalpy functions for the process of dissolution of non-polar liquids [32–34] shows that the stabilisation energy ($W_I \rightarrow W_{II}$) of water clusters is again negative and hence the process is exothermal ($\Delta H_{for} = \Delta h_{for} \cdot \xi_w < 0$) with unitary enthalpy $\Delta h_{for} = -23.3$ kJ mol^{-1} ξ_w^{-1} which is practically equal to the value obtained from gases. The extrapolated enthalpy ($\Delta H_0{}^{(\xi_w=0)} = +4.5$ kJ mol^{-1}), however, is slightly positive, indicating a small endo-thermal effect. This could be due to the energy necessary to detach the molecules from one another in the liquid phase to overcome the cohesion force. Analysis of the entropy functions confirms the large loss of entropy ($\Delta S_{for} = \Delta s_{for} \cdot \xi_w < 0$) spent to form the cavity, with unitary entropy $\Delta s_{for} = -447$ J K^{-1} mol^{-1} ξ_w^{-1}. In contrast to gases, however, the extrapolated entropy change in liquids is practically null ($\Delta S_0{}^{(\xi_w=0)} = -0.5$ J K^{-1} mol^{-1}) and is very different from the value obtained for gases and hence from that calculated by the Trouton law. We recall that the large negative value of the extrapolated entropy for gases is attributed to the loss of translational entropy of the molecules when passing from the gaseous state to the trapped state in solution. The lack of large entropy loss in the liquids is in accordance with the absence of translational entropy. In fact, the liquids, before being dissolved are already condensed.

6.3. Protein denaturation

In protein denaturation (Fig. 9), the first step of the process is the action to move the chains from the folded to the extended state [4]. This step is endo-thermal because it is energy consuming ($\Delta H_0{}^{(\xi_w=0)} = +211.8$ kJ mol^{-1}). The entropy change associated with this step is positive and large ($\Delta S_0{}^{(\xi_w=0)} + 415.8$ J K^{-1} mol^{-1}), involving a transformation of the chains from ordered to disordered state.

The next reaction step is the formation of the cavity by transforming ξ_w W_I into ξ_w $W_{II} + \xi_w$ W_{III} + cavity. This step is exothermal with $\Delta H_{for} = \xi_w \cdot \Delta h_{for} < 0$ and its unitary value per water molecule ($\Delta h_{for} = -22.1$ kJ mol^{-1} ξ_w^{-1}) is practically equal to that found in the dissolution of non-polar gases ($\Delta h_{for} = -22.6$ kJ mol^{-1} ξ_w^{-1}). In the case of proteins, however, the numbers ξ_w of water molecules are much larger and the resulting total exothermal enthalpy change ΔH_{for} is very large. The entropy change generated by the formation of the cavity is highly negative $\Delta S_{for} = \xi_w \cdot \Delta s_{for} < 0$ with unitary value per water molecule ($\Delta s_{for} = -428.5$ J K^{-1} mol^{-1} ξ_w^{-1}) practically equal to the unitary entropy change found in the dissolution of non-polar gases. Also in this case, the large number of water molecules W_{III} involved makes this step highly entropy consuming. This large entropy term ΔS_{for} will be the prominent factor in determining the thermodynamically unfavourable type of this reaction. Lastly, the water molecules W_{III} released from the cavity absorb the heat $\xi_w C_{p,w} T$ at the expense of the heat produced by the creation of the cavity and this absorbed heat is equivalent to thermal entropy $\xi_w C_{p,w} \ln T$, appropriate to the temperature T.

6.4. Protonation of carboxylato anions

In the protonation of the carboxylato anions [35–39], the total reaction (Fig. 10) can be written

$$\mathrm{R-COO^-} + \mathrm{H_3O^+} + \xi_w \mathrm{W_I} = \mathrm{R-COOH} + (\xi_w + 1)\mathrm{W_{III}} + \xi_w \mathrm{W_{II}} \qquad (21)$$

which includes the reaction (19).

The analysis of the values of the protonation constants [37,38] for seven mono-carboxylic acids has confirmed that enthalpy ΔH_{app} and entropy ΔS_{app} can be represented by Eqs. (3) and (5), respectively. For the enthalpy, we calculate the unitary value $\Delta h_{for} = -21.8$ kJ mol^{-1} ξ_w^{-1} (to be compared with $\Delta h_w = -21.6$ kJ mol^{-1} ξ_w^{-1}, for non-polar gases) for the transformation ξ_w $W_I \rightarrow \xi_w$ W_{II} and cavity formation and the value (almost nil) $\Delta H_0{}^{(\xi_w=0)} = +0.1$ kJ mol^{-1} for the extrapolated enthalpy. For the entropy, we obtain $\Delta S_{for} = \xi_w \cdot \Delta s_w < 0$ (with unitary value $\Delta s_{for} = -443$ J K^{-1} mol^{-1} ξ_w^{-1}, as compared to $\Delta s_{for} = -445$ J K^{-1} mol^{-1} ξ_w^{-1} for gas solubility) thus confirming the same very large loss of entropy for cavity formation as in non-polar gases and other processes in Class A.

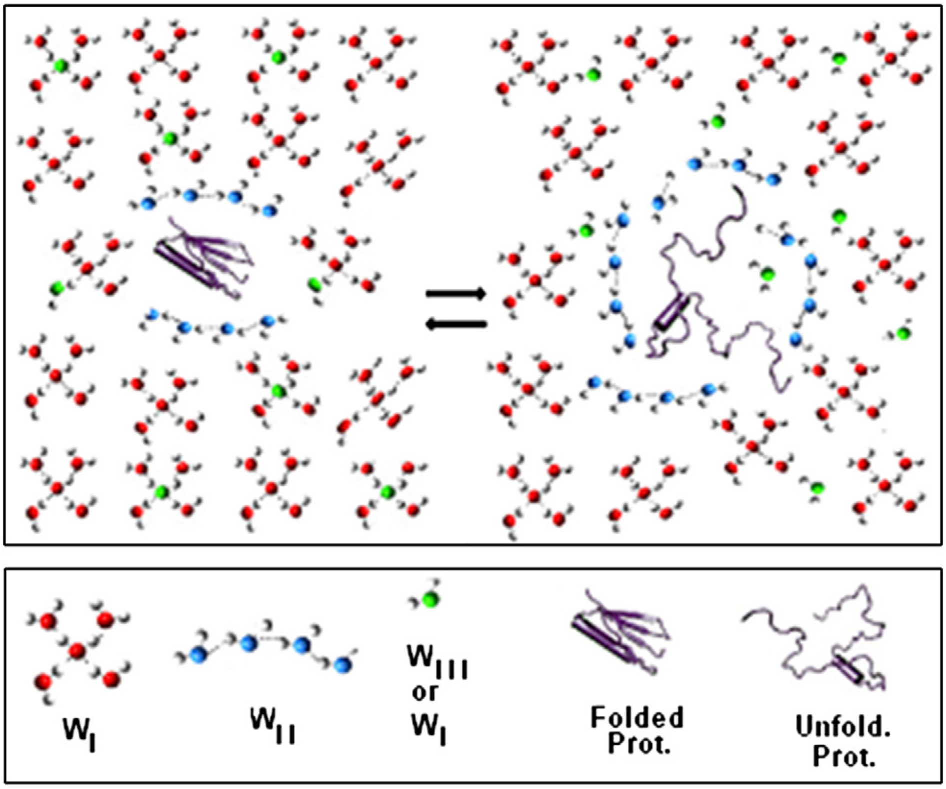

Fig. 9. Denaturation of protein.

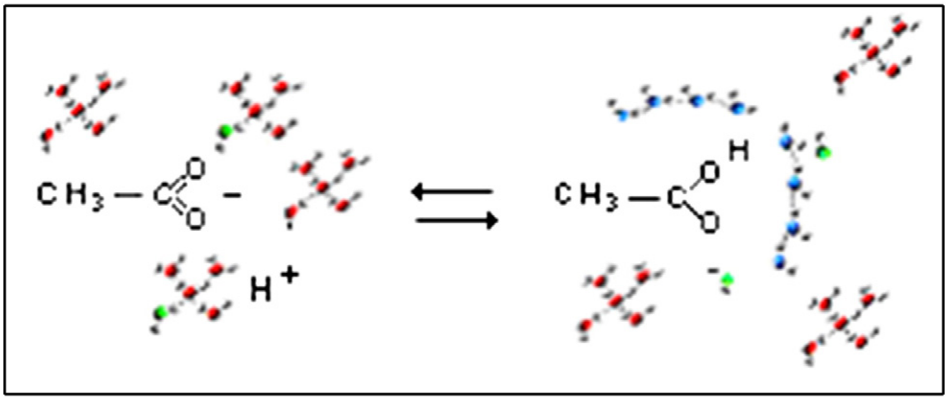

Fig. 10. Protonation of carboxylato anion.

If we calculate the values of ΔH_{calc} by Eq. (7) and of ΔS_{calc} by Eq. (8) using these unitary values $\Delta h_{for} = -21.8$ kJ mol^{-1} ξ_w^{-1} and $\Delta s_{for} = -443$ J K mol^{-1} ξ_w^{-1}, for the seven carboxylic acids at the same temperatures as the experimental points, we can calculate the values of the equilibrium constant logK_{calc} from

$$\log K_{calc} = (-\Delta G_{calc} / 2.302RT) \tag{22}$$

and then subtract these values from the experimental values logK_{app}, thus obtaining the residual

$$\Delta \log K_x \; = \; \log K_{app} - \log K_{calc}. \tag{23}$$

If we plot ΔlogK_x against $(1/T)$ in van't Hoff plots, we obtain very clear straight lines with definite slopes and intercepts, corresponding to precise values of ΔH_x and ΔS_x, respectively (Table 1). The linearity of the residual ΔlogK_x in van't Hoff plot is a further proof that the curved behaviour of the previous plot, with $\Delta C_p > 0$, was originated by the water component of the reaction. The values ΔH_x and ΔS_x of each compound can be either positive or negative. The linear behaviour indicates that these values can be referred to definite reactions. In order to identify these kinds of reactions, we have plotted the values of both ΔH_x and ΔS_x against the Hammett coefficients σ_{Ham} of the substituents. The values correlate pretty well with the Hammett coefficients. Other regularities that support this interpretation are present. In fact, the acids showing a positive enthalpy are those that are highly dissociated and that thus present a positive (endo-thermal) protonation enthalpy and a negative (endo-entropic) protonation entropy. We can, therefore, conclude that this residual constant K_x is that concerning the actual step of the association of the proton to the carboxylato anion and can be written ΔlogK_x = log K_{prot}.

Eq. (21), therefore, can be subdivided into Eq. (19) and a different protonation equilibrium, written

$$\mathrm{R-COO^- + H_3O^+ = R-COOH + H_2O} \tag{24}$$

Table 1
Residual enthalpy ΔH_x and residual entropy ΔSX_x obtained by van't Hoff plots of ΔlogK_x for carboxylic acids.

Acid	ΔH_x kJ mol^{-1}	ΔS_x J K^{-1}mol^{-1}	σ_{Ham}
Cl–ethan	9.21	−5.70	0.37
Ethan	−1.34	14.59	−0.17
CN–ethan	8.15	−13.81	0.63
Methan	−0.91	0.75	0
Propan	−0.99	17.8	−0.34
Salicylic	−3.18	−28.46	−0.36

The whole apparent constant K_{app} referring to Eq. (21) can be better written as

$$K_{app} = K_{for} \cdot K_{prot} \tag{25}$$

where K_{for} refers to Eq. (19) and K_{prot} to Eq. (24), respectively.

6.5. Class characteristics

The whole set of thermodynamic functions for processes of Class A is reported in Table 2.

The extrapolated enthalpy $\Delta H_0^{(\xi_w=0)} = -17.7$ J K^{-1} mol^{-1} of Eq. (11) corresponds to the energy of the contact complex of Eq. (17) for non-polar gases. Instead, for the dissolution of liquids, the extrapolated enthalpy is $\Delta H_0^{(\xi_w=0)} = +4.6$ J K^{-1} mol^{-1} revealing that some residual repulsion has to be overcome. In protein denaturation, the value $\Delta H_0^{(\xi_w=0)} = +211.8$ J K^{-1} mol^{-1} shows that the process of unfolding requires the expenditure of some energy. The process of protonation shows a value that is practically nil, and this is in accordance with the fact that $\Delta H_0^{(\xi_w=0)}$ refers to the constant K_{for} while the proton–anion affinity is included in the constant K_{prot}.

As already mentioned, the extrapolated entropy $\Delta S_0^{(\xi_w=0)} = -86.4$ J K^{-1} mol^{-1} of Eq. (13) for gases is coincident with the high and negative value calculated by the Trouton constant, and this is in accordance with the loss of kinetic energy by the gas when it is condensed in the cage of the solvent. When the solute is a liquid $\Delta S_0^{(\xi_w=0)}$ is practically nil because the liquid was already condensed prior to dissolution in water and there is no loss of translational entropy. In contrast, in protein denaturation there is a high positive value of $\Delta S_0^{(\xi_w=0)} = +415$ J K^{-1} mol^{-1}, probably due to the increased mobility of the unfolded chains. It is more difficult to find an explanation for the pretty high value of $\Delta S_0^{(\xi_w=0)} = +104$ J K^{-1} mol^{-1}in the protonation of carboxylic acids. One hypothesis is that this entropy increase originates from the generation of water W_{III} from the hydronium ion H_3O^+ which loses its proton.

The comparison of the thermodynamic functions for different processes evidences the striking similarity of the enthalpy and entropy values per water unit relative to cavity formation with mean values $<\Delta h_{for}> = -22.2 \pm 0.7$ kJ mol^{-1} ξ_w^{-1} and $<\Delta s_{for}> = -445 \pm 3$ J K^{-1} mol^{-1} ξ_w^{-1}. This correspondence confirms that a common mechanism exists as basis of all these processes, more precisely each of these processes is accompanied by the formation of a cavity in the solvent. The high value of the negative entropy change for cavity formation in Class A is the main contribution to the positive work free energy $\Delta G_{work} > 0$ (cf. Fig. 6) and explains the low solubility of these substances.

Table 2
Enthalpy and entropy functions for processes of Class A.

$$\Delta H_{app} = \Delta H_0^{(\xi_w=0)} + \xi_w \Delta h_{for} + \xi_w C_{p,w} T$$

$$\Delta S_{app} = \Delta S_0^{(\xi_w=0)} + \xi_w \Delta_{for} + \xi_w C_{p,w} \ln T$$

						Range of ξ_w
Enthalpy						
Gas dissolut.	$\Delta H_{app}=$	-17.7	$-21.6\cdot\xi_w$	$+\xi_w\cdot 0.0754\cdot T$	kJ mol^{-1}	2–6
Liquid dissol.	$\Delta H_{app}=$	$+4.6$	$-23.3\cdot\xi_w$	$+\xi_w\cdot 0.0754\cdot T$	kJ mol^{-1}	2.7–5.4
Protein denat.	$\Delta H_{app}=$	$+211.8$	$-22.1\cdot\xi_w$	$+\xi_w\cdot 0.0754\cdot T$	kJ mol^{-1}	80–140
Proton. carb[a]	$\Delta H_{app}=$	$+0.1$	$-21.8\cdot\xi_w$	$+\xi_w\cdot 0.0754\cdot T$	kJ mol^{-1}	1.8–2.3
Entropy						
Gas dissolut.	$\Delta S_{app}=$	-86.4	$-445.4\cdot\xi_w$	$+\xi_w\cdot 75.4\cdot \ln T$	J K^{-1} mol^{-1}	2–6
Gas (Privalov)	$\Delta S_{app}=$	-78.5 ± 23	$-450\cdot\xi_w$	$+\xi_w\cdot 75.4\cdot \ln T$	J K^{-1} mol^{-1}	
Ebull. (Trouton)	$\Delta S_{condens}=$	-86.9 ± 1.4			J K^{-1} mol^{-1}	
Liquid dissol.	$\Delta S_{app}=$	-0.5	$-447\cdot\xi_w$	$+\xi_w\cdot 75.4\cdot \ln T$	J K^{-1} mol^{-1}	2.7–5.4
Protein denat.	$\Delta S_{app}=$	$+415$	$-428.5\cdot\xi_w$	$+\xi_w\cdot 75.4\cdot \ln T$	J K^{-1} mol^{-1}	80–140
Proton. acids[a]	$\Delta S_{app}=$	$+104$	$-442.6\cdot\xi_w$	$+\xi_w\cdot 75.4\cdot \ln T$	J K^{-1} mol^{-1}	1.8–2.3
Cycl. peptides	$\Delta S_{app}=$	$+16$	$-446\cdot\xi_w$	$+\xi_w\cdot 75.4\cdot \ln T$	J K^{-1} mol^{-1}	

[a] These values refer to K_{for} in Eq. (25).

7. Validation of the model: Class B

We can now pass on to present the molecular models that explain the different processes in Class B and the peculiarities of each of them. We must recall here that (*i*) the processes of Class B are characterised by a curve $\ln K_{app} = f(1/T)$ with a maximum, (*ii*) the enthalpy vs. T is represented by a straight line with negative slope, (*iii*) the entropy vs. $\ln T$ is represented by a straight line with the same negative slope as the enthalpy, and (*iv*) the number $n_w = -\xi_w$ is negative and according to Eq. (A.2.bis) (see Appendix A) the process implies a condensation of ξ_w water molecules.

7.1. Micelle formation

In micelle formation, the standard free energy has been determined [4] as $(-\Delta G^{ø}{}_{mic})/RT = -\ln(cmc)$ by adopting a pseudo-phase model for the micelle. According to this model, the equilibrium between the monomer unit in solution and the micelle phase depends on the simple concentration in the solution phase. Neither the mass action law nor the charge of the micelle is involved. The lines are represented by Eq. (3) for enthalpy and Eq. (5) for entropy. Here again, the thermodynamic functions ΔH_{app} and ΔS_{app} were calculated from the plot $-\ln(cmc) = f(1/T)$ and found to be linearly

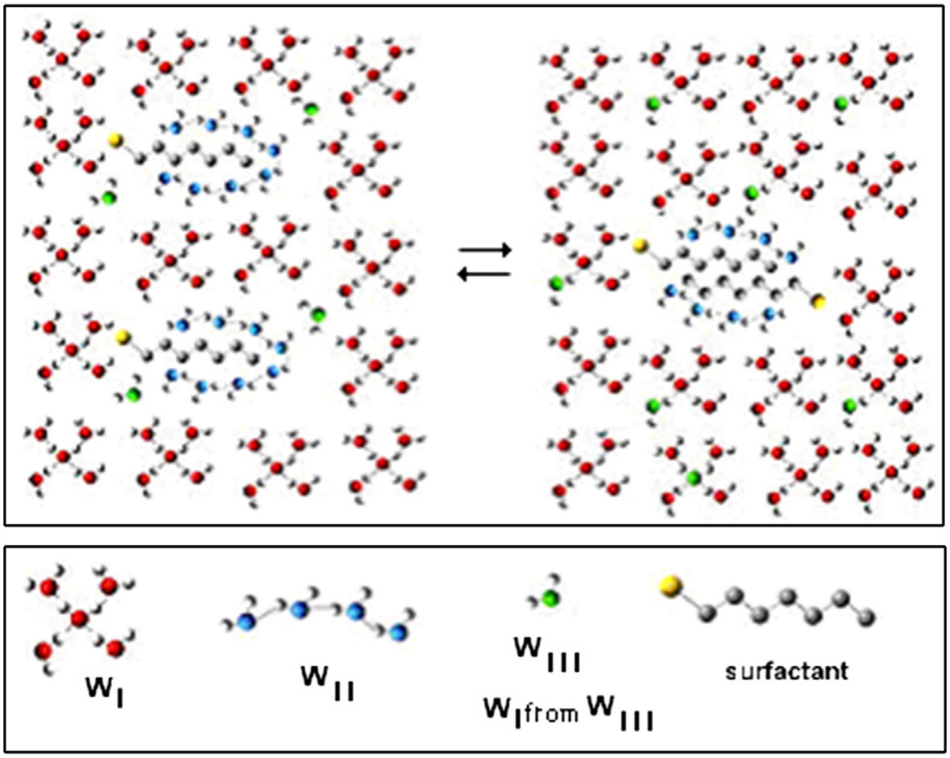

Fig. 11. Equilibrium between surfactant and micelle phase.

dependent, with identical slope ΔC_p, upon T and ln$T$, respectively. In micelle formation, however, the slope is negative, which means that in $\Delta C_p = -\xi_w C_{p,w} < 0$. This negative ΔC_p means a negative change in volume, *i.e.* reduction of cavity. In fact, we presume that the two separate units, each surrounded by a sheath of x water W_{II}, $((\text{Surf})(W_{II})_x)$ are in solution contained in their own cavity, created as in gas dissolution. When two or more such units stick to each other to form a micelle $((\text{Surf})_a(W_{II}))_{(x'+x-\xi_w)}$ (where a indicates the number of monomers already aggregated) (Fig. 11) the cavities coalesce and the resulting cavity is smaller than the sum of the volumes of the component cavities. Therefore ξ_w water molecules W_{III} return to the bulk forming again clusters W_I (regenerated from $W_{II} + W_{III}$) to fill the excess cavity. According to this approach, the exchange refers to any of the a monomer units and the coalescence of cavities takes place between the micelle $(a-1)$, with x' water units W_{II}, surrounded by its cavity and a monomer added with its own cavity. The number ξ_w, therefore, refers to the addition of the last monomer, whatever the aggregation number a.

The total process can be written

$$((Surf)(W_{II})_x) + \xi_w W_{III} + \left((Surf)_{(a-1)}(W_{II})_{x'}\right) \rightarrow \left((Surf)_a(W_{II})_{(x' + x - \xi_w)}\right) + \xi_w W_I \tag{26}$$

and corresponds to the apparent enthalpy ΔH_{app}

$$\Delta H_{app} = \Delta H_0^{(\xi_w = 0)} + \xi_w \Delta h_{red} - \xi_w C_{p,w} T. \tag{27}$$

The initial contact

$$((Surf)(W_{II})_x) + \left((Surf)_{(a-1)}(W_{II})_{x'}\right) \rightarrow ((Surf)(W_{II})_x)\left((Surf)_{(a-1)}(W_{II})_{x'}\right) \tag{28}$$

corresponds to $\Delta H_0^{(\xi_w=0)} = -3.6$ kJ mol^{-1}. This very low enthalpy change indicates the monomer–monomer affinity, which is expected to be very low. The next stepwise reaction is

$$((Surf)(W_{II})_x)\left((Surf)_{(a-1)}(W_{II})_{x'}\right) + \xi_w W_{III} \rightarrow \left((Surf)_a(W_{II})_{(x' + x - \xi_w)}\right) + \xi_w W_I \tag{29}$$

which corresponds to $\Delta h_{red} = +23.1$ kJ mol^{-1} ξ_w^{-1} indicating the heat (endothermic) needed to transform W_{II} into W_I by setting each of the ξ_w W_{III} molecules into the bulk to fill the excess cavity. Lastly, the enthalpy $-\xi_w C_{p,w} T = \Delta H_{Th}$ indicates the amount of heat (thermal enthalpy) released by ξ_w W_{III} water molecules when they are reset again into the bulk. This release of heat is analogous to a sort of crystallization or condensation heat. A negative ΔC_p, in the sense that there is an abrupt fall of C_p at *c.m.c.*, ($\Delta C_p = C_p(c.m.c.) - C_p(m) < 0 = -\xi_w C_{p,w}$) is observed in the experimental determinations of heat capacity C_p at different concentrations m of surfactant [2] and this a further proof, obtained by independent experiments, that ξ_w water molecules W_{III} are condensing at the very moment of micelle formation.

Again, the entropy can be represented, as already shown in Eq. (10), by

$$\Delta S_{app} = \Delta S_0^{(\xi_w = 0)} + \xi_w \Delta s_{red} - \xi_w C_{p,w} \ln T \tag{30}$$

where ΔS_{app} corresponds to the total reaction of Eq. (26). The term $\Delta S_0^{(\xi_w=0)} = +10.2$ J K^{-1} mol^{-1} corresponds to the partial reaction of Eq. (28) and indicates the entropy gain (dilution) by the ligand (Surf) when bound to the receptor $(\text{Surf})_{(a-1)}$, independently of the size of the ligand. The term $\Delta s_{red} = +428$ J K^{-1} mol^{-1} ξ_w^{-1} corresponding to the reaction of Eq. (29) indicates the cavity reduction equivalent to expansion of the volume of the solvent when one water molecule W_{III} is reset as bulk W_I. This entropy gain $+428\xi_w$ J K^{-1} mol^{-1} is very large and is the key thermodynamic quantity that drives the reaction. Lastly, the entropy $-\xi_w C_{p,w}$ ln T indicates the thermal entropy ΔS_{Th} released by ξ_w W_{III} water molecules when they condense back to structure W_I.

7.2. Bio-complex formation

The complexes formed by ligands and substrates with proteins show interesting properties strictly connected with the process of micelle formation. The equilibrium constant of calf brain microtubules has been determined by Timasheff et al. [40,41] at different temperatures. The diagram (cf. Fig. 3) presents a curve with upward convexity with a maximum, the opposite of what we found for the solubility of non-polar substances and the same as we found in micelle formation. The tangent to the curve (*i.e.* $-\Delta H_{app}/R$) goes from a positive value at high temperatures (exothermic) to a negative value (endothermic) at low temperatures. Plotted against T, ΔH_{app} produces a line whose slope is negative ($\Delta C_p < 0$). The equilibria of *lac* repressor [42] show analogous behaviour with a symmetric operator system and also *Eco*RI endonuclease [42] with its specific recognition site. The apparent enthalpy can be represented by the equation

$$\Delta H_{app} = \Delta H_0^{(\xi_w = 0)} + \xi_w \Delta h_{red} - \xi_w C_{p,w} T \tag{31}$$

with $\Delta H_0^{(\xi_w=0)} = -120.9$ kJ mol^{-1}, $\Delta h_{red} = +24.32$ kJ mol^{-1}, and $C_{p,w} = 0.07536$ kJ K^{-1} mol^{-1}, and by substitution

$$\Delta H_{app} = -120.9 + 24.32\xi_w - \xi_w C_{p,w} T \tag{32}$$

with $\Delta H_{red} = \xi_w \cdot h_{red} = 24.32$ $\xi_w > 0$ representing the energy to be spent to reduce the cavity. The last term of the r.h.s. represents the thermal enthalpy, ΔH_{Th} lost by ξ_w water molecules W_{III}, when they condense back to structure W_I. Many more protein complexes conform to the model, as shown in Table 7 of Ref. [2]. A process analogous to that of micelle formation can be invoked (Fig. 12). Before association, the chains of the site of the macromolecule are immersed in their cavity as well as the ligand. When macromolecule and ligand approach each other, the cavities coalesce and the resultant cavity is smaller than the sum of the two separate cavities. Hence, ξ_w water molecules W_{III} go back to structure W_I. The values of ξ_w obtained in the formation of the complexes are much larger than those found with micelle formation.

In analogy with the gas dissolution process, we analysed the entropy values for complex formation. The entropy values ΔS_{app} plotted against ln$T$ give straight lines, conform to Eq. (5), with different slopes for each compound. The slopes of $\Delta H = f(T)$ and $\Delta S = f$ (ln$T$) plots are identical for each compound.

In other words, if we plot the slopes $m_{(S)}$ for protein complexes against ξ_w determined from the plot $\Delta H = f(T)$, we obtain a straight line with proportionality factor 75.5 (cf. molar heat capacity of water $C_{p,w} = 75.36$ J K^{-1} mol^{-1}, used in calculating ξ_w from the enthalpy change). Therefore, the apparent entropy confirms that also in protein complexes (as for the solubility of non-polar gases)

$$\Delta S_{Work} = \Delta S_0^{(\xi_w = 0)} + 436.2\xi_w \text{J K}^{-1}\,\text{mol}^{-1} \tag{33}$$

represents the increase in entropy caused by occupation of part of the cavity, and the term -75.5 ξ_w ln$T$ represents the thermal entropy, ΔS_{Th} lost by ξ_w condensed water molecules W_{III}. We note that the entropy change depends on $\Delta C_p = -C_{p,w}$ $\xi_w < 0$. Therefore, the apparent entropy can be represented by the equation

$$\Delta S_{app} = \Delta S_{Work} - 75.5\xi_w \ln T \tag{34}$$

where the term ΔS_{Work} (>0), depending on the cavity volume and hence proportional to ξ_w, the unitary entropy gain, per water molecule W_{III}, $\Delta s_{red} = 436.2$ J K^{-1} mol^{-1} ξ_w^{-1} is very close to the value $\Delta s_{red} = 428$ J K^{-1} mol^{-1} ξ_w^{-1} found in micelle formation, thus

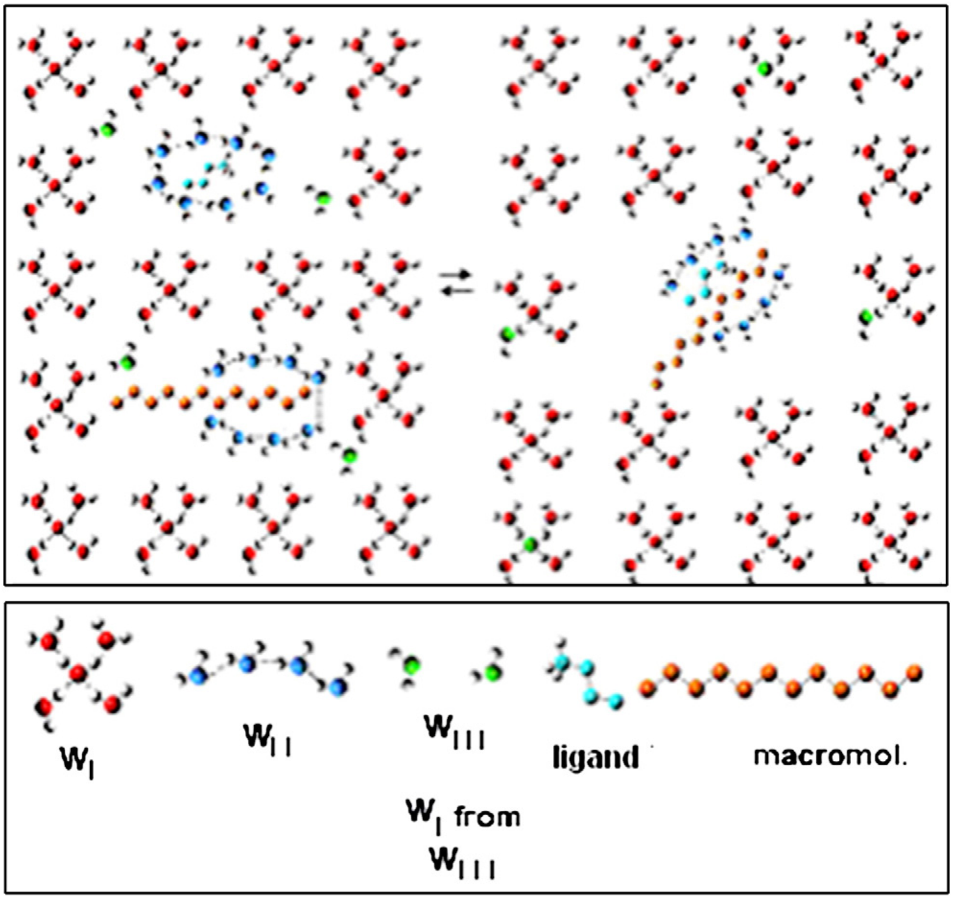

Fig. 12. Mechanism of complex formation between a macromolecule and a ligand.

confirming further the close analogy between the two types of processes. The term $\Delta S_0^{(\xi_w=0)} = +262\ \mathrm{J\,K^{-1}\,mol^{-1}}$ could be due to further entropy gain dependent not so much on cavity reduction volume as on the dilution of the ligand. This dilution takes place because the portion of ligand bound disappears as independent molecular unity from the solution. In this regard, dilution is a measure of an affinity constant.

7.3. Effect of polar group

The effect of polar group cannot be determined by measurements of some equilibrium constant but only by enthalpy change determined by calorimetry. Cabani et al. [43,44] have reported a long list of compounds for which the values of ΔC_p have been determined by calorimetry by measuring ΔH at different temperatures. The values of ΔC_p can be transformed into values of ξ_w by division by $C_{p,w}$. Cabani et al. searched for a composition rule of ΔC_p. They proposed a formula

$$\Delta C_p = A_Z + \Sigma_j n_j B_Z(j) \tag{35}$$

where A_Z is a general extrapolation constant. They attributed to each group or moiety of a molecule a typical constant contribution $B_Z(j)$, and n_j is the number of times that the j-th group appears in the molecule. Translated into our convention (Table 3), this corresponds to assigning a value $\Delta\xi_w(j) = B_Z\ (j)\ /C_{p,w}$ to each portion of the molecule. Cabani et al. divided the coefficients into two categories, one for non-polar groups with positive coefficients and another for polar groups or components with negative coefficients. All the coefficients can be transformed into values of $\Delta\xi_w$. The positive coefficients for non-polar groups are indicative of the same effect (*i.e.* formation of a cavity and cage with expulsion of water W_{III}) on the surrounding solvent as the reactions of Class A. In contrast, the negative coefficients of polar groups, transformed into values of $\Delta\xi_w$, indicate that the presence of polar groups in the molecules yields the same transformation of the water molecules of the solvent as that produced by micellisation or bio-complex formation. In the latter cases, the reduction of the cage occurring when two hydrophobic chains become close to each other causes the condensation of ξ_w water molecules W_{III} to join water W_{II} to reproduce water W_I, *i.e.* volume of solvent.

It is worth noting that the passage from fluoro-substitution to chloro-, bromo-, or iodo-substitution produces a change from $\Delta\xi_w = -0.4$ for F, to

Table 3
Group contributions to ΔC_p.

Group	B_z (J K^{-1} mol^{-1})	$\Delta\xi_w$	Group	B_z (J K^{-1} mol^{-1})	$\Delta\xi_w$
CH_3	6.4	0.881	NH_2	−75.5	−1.002
CH_2	64.5	0.856	NH	−7.7	−0.102
CH	67.8	0.899	N	−39.0	−0517
C	44.7	0.593	N_{ar}	−12.0	−0.159
C==C	100.8	1.337	O	−62.6	−0.830
C==–C	44.5	0.588	OH	−44.4	−0.589
$CH_{2,cycl}$	47.3	0.628	SO	−152.0	−20.17
CH_{ar}	26.0	0.345	F	−30.3	−0.402
C_{ar}	0.0	0.000	Cl	2.0	0.027
C_{cond}	0.1	0.001	Br	18.4	0.244
CHO	−91.0	−1.207	I	235.2	3.120
CO	−79.5	−1.055	NHCONH	−81.0	−1.075
COO	−37.0	−0.491	NH_2CON	−99.9	−1.325
COOH	−84.7	−1.124	NCON	−88.4	−1.173
$CONH_2$	−84.6	−1.122	OH(Φ)	−32.3	−0.429
CONH	−87.4	−1.159		A_z (J K^{-1} mol^{-1})	$\Delta\xi_w$
CON	−112.4	−1.491		115.9	1.538

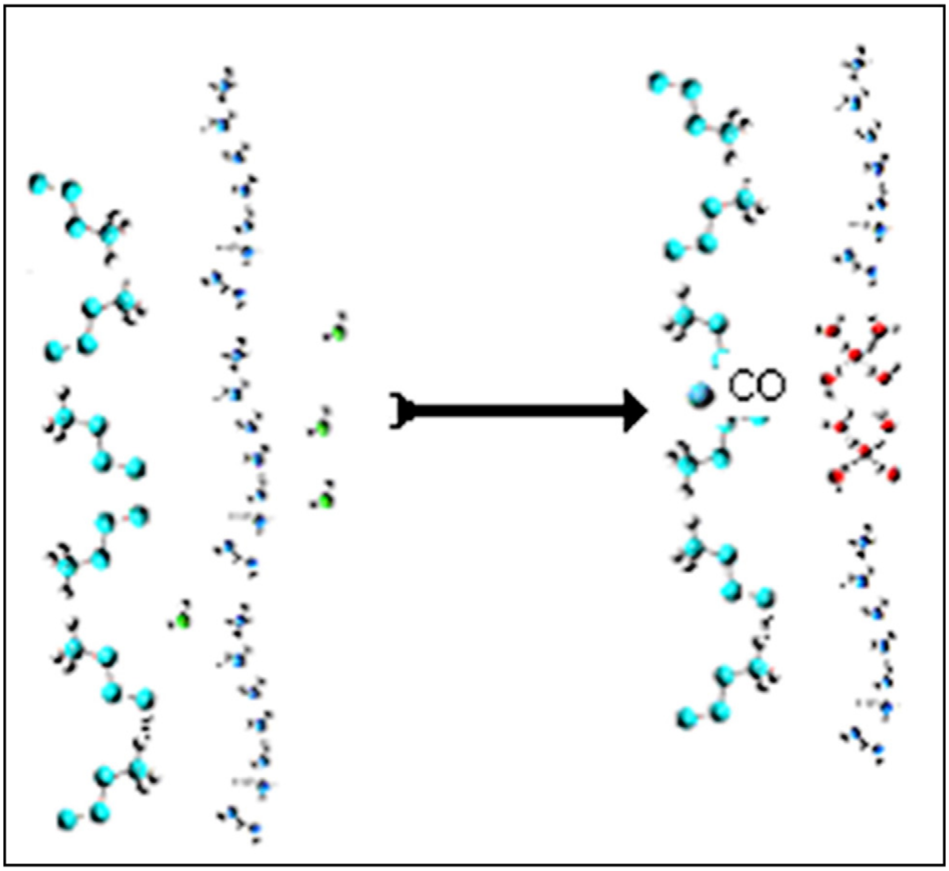

Fig. 13. Effect of introduction of a polar group into a hydrophobic chain. Introduction of the polar group produces the transformation B$(-\xi_w W_{II} - \xi_w W_{III} \rightarrow \xi_w W_I - \text{cavity})$.

$\Delta\xi_w = +0.03$ for Cl, to $\Delta\xi_w = +0.24$ for Br, and to $\Delta\xi_w = +3.12$ for I. This fact underlines the effect of solute polarity on the structure of the surrounding solvent. The strong electronegative fluorine molecule promotes the condensation of water molecules as in micelle formation whereas the weak-electronegative iodine facilitates the expulsion of W_{III} and the formation of a cavity. Substitution of a part of the hydrocarbon molecule with a polar moiety, as for example $=$CO (Fig. 13), produces the transformation $(\xi_w W_{III} + \xi_w W_{II-} \rightarrow \xi_w W_I - \text{cavity})$ typical of Class B.

7.4. Introduction of a negative charge

The introduction of a negative charge is exemplified by the process opposite to protonation, already described for Class A. Dissociation of a proton produces the process of reducing the cavity with transformation $(-\xi_w W_{III} - \xi_w W_{II} \rightarrow \xi_w W_I - \text{cavity})$ typical of the processes of Class B.

7.5. Hydrophobic association (so-called "hydrophobic bond")

The hydrophobic association is exemplified by the association between two aliphatic chains to form a micelle. The driving force is clearly an entropy-producing effect due to filling of the excess cavity derived from the close association of the aliphatic moieties. By calculating the motive or work free energy, the negative free energy is definitely found to be a consequence of the highly positive entropy production. In fact, the entropy gain $+428\xi_w$ J K^{-1} mol^{-1} is very large and is the key thermodynamic quantity that drives the reaction.

7.6. Class characteristics

The complete set of enthalpy and entropy values can be found only for micelle and bio-complex formation (Table 4). The term $\Delta H_0^{(\xi_w=0)} = -4.22$ kJ mol^{-1} indicates the very low affinity between two hydrophobic

Table 4
Enthalpy and entropy functions for processes of Class B.

$$\Delta H_{app} = \Delta H_0^{(\xi_w = 0)} + \xi_w \Delta h_{red} – \xi_w C_{p,w} T$$

$$\Delta S_{app} = \Delta S_0^{(\xi_w = 0)} + \xi_w \Delta s_{red} – \xi_w C_{p,w} \ln T$$

						Range of ξ_w
Enthalpy						
Micelle	$\Delta H_{app}=$	-4.22	$+23.2 \cdot \xi_w$	$-\xi_w \cdot 75.4 \cdot T$	kJ mol^{-1}	4–19
Bio-complx	$\Delta H_{app}=$	-120.9	$+24.3 \cdot \xi_w$	$-\xi_w \cdot 75.4 \cdot T$	kJ mol^{-1}	19–189
Entropy						
Micelle	$\Delta S_{app}=$	$+10.2$	$+428 \cdot \xi_w$	$-\xi_w \cdot 75.4 \cdot \ln T$	J K^{-1} mol^{-1}	4–19
Bio-complx	$\Delta S_{app}=$	$+262$	$+436.2 \cdot \xi_w$	$-\xi_w \cdot 75.4 \cdot \ln T$	J K^{-1} mol^{-1}	19–189

moieties; the same term $\Delta H_0^{(\xi_w=0)} = -120.9$ kJ mol^{-1} for bio-complex formation is much higher and indicates the existence of some affinity between receptor and ligand. The unitary enthalpy change for cavity filling is positive and practically equal in the two types of reactions (mean $<\Delta h_{red}> = 23.7 \pm 0.6$ kJ mol^{-1} ξ_w^{-1}). It indicates that restoring of the structure of water is energy consuming, the opposite of that for cavity creation, which is energy producing.

As for the entropy, the extrapolated term for micelle $\Delta S_0^{(\xi_w=0)} = +10.2$ J K^{-1} mol^{-1} indicates a favorable small entropy production which is much higher for bio-complex formation, $\Delta S_0^{(\xi_w=0)} = +262$ J K^{-1} mol^{-1}. The unitary entropy change for cavity reduction is very high for both types of reactions and almost equal in the two types ($\Delta s_w = +432 \pm 4$ J K^{-1} mol^{-1} ξ_w^{-1}). The coincidence of unitary values for cavity reduction both for enthalpy and for entropy is a strong indication of the validity of the model. Again, by recalling the separation between thermal and work components, we can calculate the work free energy $\Delta G_{Work} < 0$ of complex formation (cf. Eq. (16)) where the entropy term ($-T\Delta S_{Work} < 0$) is the main contributor to the affinity of the association (cf. Fig. 7). All the processes of Class B, whenever entropy values are available, clearly result as being entropy-driven.

8. Comparison between Classes

The values of the stepwise thermodynamic functions of Class A present very interesting connections with those of Class B (Table 5). The comparison can be better performed by taking the process of gas dissolution as representative of Class A and the process of micelle formation as representative of Class B. The two Classes are strictly connected. In fact, the thermodynamic functions ΔH_{app} and ΔS_{app} in both Classes can each be broken down into three terms, each of which can be assigned to a specific reaction step. In enthalpy (Table 5, 1) the values of the first term $\Delta H_0^{(\xi_w=0)} = -17.7$ kJ mol^{-1} for gas in water and $\Delta H_0^{(\xi_w=0)} = -3.6$ kJ mol^{-1} for micelle are indicative of the attraction between gas and solvent in the former and between two monomer units in the latter. The different entities, notable in Class A and very low in Class B, meet all expectations reasonably well. The second term $\xi_w\ \Delta h_{for}$ is bound to the formation of the cavity (exothermal) in Class A ($\Delta H_{for} = \xi_w\ \Delta h_{for} < 0$) or to a reduction in the cavity (endothermal) in Class B ($\Delta H_{red} = \xi_w\ \Delta h_{red} > 0$). The reaction is the same *i.e.* dissociation $\mathbf{A}(\xi_w W_I \rightarrow \xi_w W_{II} + \xi_w W_{III} + \text{cavity})$ in Class A and the reverse reaction $\mathbf{B}(\xi_w W_{II} + \xi_w\ W_{III} \rightarrow \xi_w W_I - \text{cavity})$ in Class B. It is worth noting that the unitary values $\Delta h_{for} = -21.6$ kJ mol^{-1} ξ_w^{-1} in gas dissolution and $\Delta h_{red} = +23.1$ kJ mol^{-1} ξ_w^{-1} in micelle formation are practically equal, apart from the sign which is, of course, opposite. It is also noteworthy that the two processes of gas dissolution and micelle formation are good representatives of the respective Classes. In fact, values very close to these are the mean values in each Class: for Class A we calculate the mean $<\Delta h_{for}> = -22.2 \pm 0.7$ kJ mol^{-1} ξ_w^{-1} and for Class B the mean $<\Delta h_{red}> = 23.7 \pm 0.6$ kJ mol^{-1} ξ_w^{-1}.

One more point can be put in evidence. The enthalpy value $<\Delta h_{for}> = -22.2 \pm 0.7$ kJ mol^{-1} ξ_w^{-1} corresponds exactly to the energy of a hydrogen bond ($\Delta H_{HB} = -22.2$ kJ mol^{-1}) [26]. This result leads us to re-examine the different proposals for the structure of liquid water. The most satisfactory model is the so-called "mixture model" [5,6], with the possible existence, together with the two species in equilibrium, of interstitial water molecules, entering the spaces of the structure. These free water molecules could correspond to the molecules W_{III}. The two species in equilibrium in liquid water, could be identified as W_I and W_{II}, respectively. The difference between W_I and W_{II} could consist in the different strength of the hydrogen bonds in the two types of clusters. In clusters W_I, there could be two weak hydrogen bonds, summing up to the enthalpy $\Sigma(\Delta H_{HB}) = -22$ kJ mol^{-1}, whereas in the clusters W_{II} there could be two strong hydrogen bonds summing up to the enthalpy $\Sigma(\Delta H_{HB}) = -44$ kJ mol^{-1}. The resulting difference would be $(\Delta H_{HB}) = -22$ kJ mol^{-1} corresponding to $<\Delta h_{for}>$.

The third term $\pm \xi_w C_{p,w} T$ kJ mol^{-1} corresponds to heat absorbed by ξ_w water molecules W_{III} that are relaxed by the structure in Class A

Table 5
Correspondence between thermodynamic terms in the two Classes A and B.

Themodyn. term	Value	Chemical reaction	Physical–*chemical process*
1) Enthalpy			
A) non-polar gas dissolution ($n_w > 0$) ($\xi_w = \lvert n_w \rvert$)			
$\boldsymbol{\Delta H_{app} = \Delta H_0^{(\xi_w=0)} + \xi_w \Delta h_{for} + \xi_w C_{p,w}\ T}$			
$\Delta H_0^{(\xi_w=0)}$ /kJmol^{-1}	−17.7	$(Kr)_{Gas} + \xi_w\ W_I \rightarrow (Kr)(W_I)_{\xi w}$	Gas–water affinity
Δh_{for} /kJ mol^{-1} ξ_w^{-1}	−21.6	$(Kr)(W_I)_{\xi w} \rightarrow (Kr)(W_{II})_{\xi w} + \xi_w\ W_{III}$	Energy emitted in Cavity formation
$\xi_w\ C_{p,w}\ T$/kJ mol^{-1}	>0	$(-\xi_w\ W_I\ )_{struct} \rightarrow \xi_w\ W_{III}$	Heat absorbed by ξ_w W_{III} molec. released
B) Micelle formation ($n_w < 0$) ($\xi_w = \lvert n_w \rvert$)			
$\boldsymbol{\Delta H_{app} = \Delta H_0^{(\xi_w=0)} + \xi_w \Delta h_{red} - \xi_w C_{p,w}\ T}$			
$\Delta H_0^{(\xi_w=0)}$/kJ mol^{-1}	−3.6	$2(alk)(W_{II})_x \rightarrow (alk)_2(W_{II})_{2x}$	Monomer–monomer affinity (low)
Δh_{red}/kJ mol^{-1} ξ_w^{-1}	+23.1	$-\xi_w\ W_{III} + (alk)_2(W_{II})_{2x} \rightarrow (alk)_2(W_{II})_{2x-\xi w} + \xi_w\ W_I$	Energy absorbed in Cavity reduction
$-\xi_w C_{p,w}\ T$/kJ mol^{-1}	<0	$-\xi_w\ W_{III} \rightarrow (\xi_w\ W_I\ )_{struct}$	Heat released by ξ_w W_{III} molec. restructured
2) Entropy			
A) Non-polar gas dissolution ($n_w > 0$) ($\xi_w = \lvert n_w \rvert$)			
$\boldsymbol{\Delta S_{app} = \Delta S_0^{(\xi_w=0)} + \xi_w \Delta s_{for} + \xi_w C_{p,w}}$ ln $\boldsymbol{T}$			
Themodyn. term	Value	Chemical reaction	Physical–chemical process
$\Delta S_0^{(\xi_w=0)}$/J K^{-1} mol^{-1}	−86.4	$(Kr)_{Gas} + \xi_w\ W_I \rightarrow (Kr)(W_I)_{\xi w}$	Configurational entropy lost by gas trapped
Δs_{for}/J K^{-1} mol^{-1} ξ_w^{-1}	−445	$(Kr)(W_I)_{\xi w} \rightarrow (Kr)(W_{II})_{\xi w}$	Entropy loss in Cavity formation
$n_w C_{p,w}$ ln T/J mol^{-1}	>0	$-\xi_w\ W_I \rightarrow \xi_w\ W_{III}$	Thermal entropy gained by ξ_w W_{III} molec. released
B) micelle formation ($n_w < 0$) ($\xi_w = \lvert n_w \rvert$)			
2) $\boldsymbol{\Delta S_{app} = \Delta S_0^{(\xi_w=0)} + \xi_w \Delta s_{red} - \xi_w C_{p,w}}$ ln $\boldsymbol{T}$			
$\Delta S_0^{(\xi_w=0)}$/J K^{-1} mol^{-1}	+10.2	$2(alk)(W_{II})_x \rightarrow (alk)_2(W_{II})_{2x}$	Configurational entropy gain by ligand
Δs_{red}/J K^{-1} mol^{-1} ξ_w^{-1}	+428	$-\xi_w W_{III} + (alk)_2(W_{II})_{2x} \rightarrow (alk)_2(W_{II})_{2x-\xi w} + \xi_w W_I$	Entropy gain in Cavity reduction
$-\xi_w C_{p,w}$ ln T/J K^{-1} mol^{-1}	<0	$-\xi_w\ W_{III} \rightarrow \xi_w\ W_I$	Thermal. entropy lost by ξ_w W_{III} molec. restructured

$(+\xi_w C_{p,w}\ T)$ whereas in Class B $(-\xi_w C_{p,w}\ T)$ it represents the same amount of heat lost by ξ_w water molecules W_{III} that are condensed again in the structure of the bulk. The two processes are the opposite of each other, in a similar way to boiling and condensation. As far as entropy is concerned (Tables 5, 2), the first term is again associated with the first step of the reaction. In fact, we find for $\Delta S_0^{(\xi_w=0)} = -86.4\ \mathrm{J\,K^{-1}\,mol^{-1}}$ a value (cf. Trouton law) corresponding exactly to the kinetic energy lost by a gas molecule when it becomes trapped in the cage of solvent.

In Class B, the first term indicates a positive entropy change, $\Delta S_0^{(\xi_w=0)} = +10.2\ \mathrm{J\,K^{-1}\,mol^{-1}}$, produced by dilution of the solute when it disappears from the solution becoming associated with the rest of the micelle. The second term of entropy is, similarly to enthalpy, associated with the cavity formation in Class A ($\Delta S_{for} = \xi_w\ \Delta s_{for} < 0$) or with the cavity reduction in Class B ($\Delta S_{red} = \xi_w\ \Delta s_{red} > 0$). Here again the values are almost equal but with reversed sign: in Class A we find $\Delta s_{for} = -445\ \mathrm{J\,K^{-1}\,mol^{-1}}\,\xi_w^{-1}$ for cavity formation and in Class B we find $\Delta s_{red} = +428\ \mathrm{J\,K^{-1}\,mol^{-1}}\,\xi_w^{-1}$ for cavity reduction. The coincidence of values with opposite signs is a further proof of the validity of the molecular model proposed. As seen for enthalpy, the two processes of gas dissolution and micelle formation are good representatives of the respective Classes with mean value $\langle\Delta s_{for}\rangle = -445 \pm 3\ \mathrm{J\,K^{-1}\,mol^{-1}}\,\xi_w^{-1}$ in Class A and mean $\langle\Delta s_{red}\rangle = +432 \pm 4\ \mathrm{J\,K^{-1}\,mol^{-1}}\,\xi_w^{-1}$ in Class B.

Lastly, the third term of entropy refers to the thermal entropy $\Delta S_{Th} = \xi_w C_{p,w}\ \ln T\ \mathrm{J\,K^{-1}\,mol^{-1}}$ as for enthalpy, associated with the passage of state of water W_{III} and represents in Class A the thermal entropy gained by these water molecules W_{III} when they reach the thermal level appropriate to the temperature T. In Class B, the entropy change $\Delta S_{Th} = -\xi_w C_{p,w}\ \ln T\ \mathrm{J\,K^{-1}\,mol^{-1}}$, corresponding to the third term, represents the same kinetic energy, lost as heat released to the surroundings, by the water molecules W_{III} when they become condensed again in the bulk.

9. Conclusions

Analysis of the thermodynamic functions of hydrophobic hydration processes, examined under the light of *TED* principle, allowed us to find the close analogies that underlie all these apparently different processes. The molecular [1,2] mechanism of the hydrophobic hydration processes can be successfully interpreted by assuming a particular structure for liquid water. Liquid water consists of two types of clusters W_I and W_{II} and of free water molecules W_{III}. Application of *TED* principle has enabled the determination of the stoichiometric coefficient ξ_w of water W_{III}, in every process. The hydrophobic hydration processes can be subdivided into two Classes: A and B, whereby the same reaction in opposite directions takes place, respectively. In Class A there is the cavity formation with the dissociation of ξ_w water molecules W_{III}, whereas in Class B there is the cavity reduction with condensation of ξ_w water molecules W_{III}. The number ξ_w is different in the various processes and is proportional to the size of the reacting molecules. Analysis of the thermodynamic functions has yielded numerical values of the functions themselves that are self-consistent and perfectly coherent with the molecular model assumed. In particular, the unitary values of enthalpy and entropy relative to cavity formation and cavity reduction form a self-consistent scheme (Table 6), using mean values $\langle\Delta h\rangle$ and $\langle\Delta s\rangle$ for each Class. The consistency of these data gives further support to the reliability of the model.

Table 6
Comparisons of mean unitary thermodynamic functions in Class A and Class B.

	Cavity	Water W_{III}	$\langle\Delta h\rangle$ ($\mathrm{kJ\,mol^{-1}}\,\xi_w^{-1}$)	$\langle\Delta s\rangle$ ($\mathrm{J\,K^{-1}\,mol^{-1}}\,\xi_w^{-1}$)
Class A	Formation	→ W_{III} from W_I	-22.2 ± 0.7	-445 ± 3
Class B	Reduction	→ W_{III} to W_I	$+23.7 \pm 0.6$	$+432 \pm 4$

A surprising feature of these unitary mean values is that they have been calculated by including results obtained from both large and small molecules. This indicates that the same type of unitary reaction is taking place in every case, independently from the total size of the reactant. This result is very important because it is in contrast with some theories supported by molecular calculations [45,46] that retain that the hydrophobic character of the macromolecule would be associated to a special situation induced in the solvent at the external surface of the macromolecule. In contrast, small molecules would be allocated within the interstices of the solvent. The passage from one another type of organisation of the solvent would take place at a specific cross-over point that can be calculated by an appropriate algorithm. Actually, according to our model, the type of transformation in the solvent is the same both in small and large molecules. In fact, we remind that the number ξ_w is proportional to the volume of the cavity receiving the solute or, in the denatured macromolecules, to the volume of the cavity allocating the unfolded chains. The number of unfolded chains is proportional to the external surface of the macromolecule and this fact has induced many researchers to accept the over mentioned theory. Actually, according to our model, there is no cross-over point, at least in the solvent structure. We can recognise, instead, a cross-over point concerning the solute, in the passage from solubility process to denaturation process. In fact, the phenomenon of cavity formation involves the whole molecule in the solubility of gases and liquids but only the external chains in the denaturation process.

The finding that so many reactions can be viewed as the same direct or inverse type of transformation with equal unitary energetics, independent from the size of the reactant, should be relevant for Biological Physical Chemistry. Cavity formation or reduction seems to be ubiquitous in aqueous solutions. This fact should encourage the search for the molecular basis of many biological processes, which is the ultimate aim of Biological Physical Chemistry and of Biological Thermodynamics.

A further merit of the proposed model is that the results found confirm the validity of suggestions and observations published by several authors, namely Ben-Naim [9], Guillot and Giussani [11], Lee and Graziano [12], Lumry [22,23], Winzor and Jackson [24], Nemethy and Sheraga [47], Widom et al. [48], Sharp and Madam [49,50], Pohorille and Pratt [51], among others. Each of them has caught, either by experiments or by molecular calculations, some single step of the whole process: (*i*) cavity formation or (*ii*) cavity reduction, (*iii*) entropy/enthalpy compensation, (*iv*) a type of water dispersed in the interstices similar to W_{III}, (*v*) motive and thermal functions (*vi*) types of water clusters similar to W_I and W_{II}, respectively, (*vii*) formation of clathrate type cages around the solute comparable to the function of water W_{II}. It seems to us that every one of these aspects has now been settled within a framework of a comprehensive model. Unfortunately, none of the many molecular calculations has taken into account the substantial separation of work and thermal parts of the thermodynamic functions, thus developing algorithms for the hydrophobic effect that do not represent the real situation.

Acknowledgements

Professor G. Chiusoli, Emeritus, is kindly thanked for his invaluable help in the presentation of the paper.

This work was supported by the contributions from the Fondazione Cassa di Risparmio di Parma and from the University of Parma.

Appendix A. Equilibrium constant and thermodynamic relationships

For a correct thermodynamic treatment of hydrophobic hydration, we assume that, for processes of Class A, the constant K_{app} experimentally determined is bound to the true constant $K_{(0)}$ by a factor depending on the equivalent thermal activity of water W_{III}, $[(W_{\mathrm{III}})_T]$ (see Appendix B)

$$K_{app} = K_{(0)}\left[(W_{\mathrm{III}})_T\right]^{-\xi_w} \tag{A.1}$$

where ξ_w is a positive number indicating the number of water molecules W_{III} involved in the process. We observe that by rewriting Eq. (A.1) as

$$K_{(0)} = K_{app}\left[(W_{\mathrm{III}})_T\right]^{\xi_w} \tag{A.1.bis}$$

the true constant $K_{(0)}$ appears as a sort of dissociation constant of a reaction whereby ξ_w water molecules are dissociated. In contrast, for the processes of Class B an equilibrium constant

$$K_{app} = K_{(0)}\left[(W_{\mathrm{III}})_T\right]^{\xi_w} \tag{A.2}$$

can be assumed whereby the true constant $K_{(0)}$ becomes a condensation constant with respect to water molecules

$$K_{(0)} = K_{app}\left[(W_{\mathrm{III}})_T\right]^{-\xi_w} \tag{A.2.bis}$$

On the basis of the dissociation equilibrium of Eq. (A.1) and of the opposite condensation equilibrium of Eq. (A.2), a complete algebra of the thermodynamic functions can be developed.

For the reactions of Class A, by taking the logarithms of Eq. (A.1), we obtain

$$RT\ln K_{app} = RT\ln K_{(0)} - \xi_w RT\ln\left[(W_{\mathrm{III}})_T\right] \tag{A.3}$$

By derivation of $\ln K_{app} = (-\Delta G°/RT)$ with respect to $(1/T)$ we obtain Eq. (2) (van't Hoff equation).

On the other hand, by calculating as in Eq. (2) the derivative of Eq. (A.3) with respect to $(1/T)$, we obtain

$$\partial(\ln K_{app})\,/\,\partial(1\,/\,T) = \partial\left(\ln K_{(0)}\right)/\,\partial(1\,/\,T) - \xi_w\partial\ln\left[(W_{\mathrm{III}})_T\right]\partial(1\,/\,T) \tag{A.4}$$

The last term of this equation can be rearranged as

$$-\xi_w\partial\ln\ \left[(W_{\mathrm{III}})_T\right]\partial(1\,/\,T) = \xi_w T\partial\ln\ \left[(W_{\mathrm{III}})_T\right]/\,\partial\ln T \tag{A.5}$$

and then, by recalling *TED* principle (see Appendix B)

$$-\xi_w R\mathrm{d}\ln\left[(W_{\mathrm{III}})_T\right] = \xi_w C_{p,w}\mathrm{d}\ln T \tag{A.6}$$

we obtain

$$-\partial(\ln K_{app})\,/\,\partial(1\,/\,T) = \Delta H_0\,/\,R + \xi_w C_{p,w}T\,/\,R \tag{A.7}$$

This means that the thermodynamic function ΔH_{app} obtained from the tangent to the curve in the diagram $\ln K_{app} = f(1/T)$, is represented by a straight line

$$\Delta H_{app} = \Delta H_{Work} + \xi_w C_{p,w}T \tag{A.8}$$

with slope

$$\Delta C_p = \xi_w C_{p,w} \tag{A.9}$$

Eq. (A.8) corresponds to Eq. (3) and supports theoretically what had been calculated directly from the experimental data. The tangent of the curve, $(-\Delta H_{app}/R)$, for compounds or processes of Class A goes from positive values $(-\Delta H_{app}>0)$ at low temperatures (cf. portion of the curve to the right of the minimum in Fig. 2) to negative values $(-\Delta H_{app}<0)$ at high temperatures (cf. portion of the curve to the left of the minimum in Fig. 2). The values of the enthalpy change ΔH_{app} go the opposite way, from negative to positive values with increasing temperatures, passing through a temperature at which ΔH_{app} is nil and the process is adiabatic.

Alternatively for processes of Class B, we can calculate the same set of equations as from Eqs. (A.4) to (A.7) with exponent $-\xi_w$ thus obtaining an expression for enthalpy

$$\Delta H_{app} = \Delta H_{Work} - \xi_w C_{p,w}T \tag{A.10}$$

obtained from the experimental data. In fact, the tangent of the curve for compounds or processes of Class B goes from negative values $(-\Delta H_{app}<0)$ at low temperatures, (cf. portion of the curve to the right of the maximum in Fig. 3) to positive values $(-\Delta H_{app}>0)$ at high temperatures (cf. portion of the curve to the left of the maximum in Fig. 3).

On the other hand, starting from the Helmholtz equation,

$$\partial(-\Delta G^{\circ}{}_{app})\,/\,\partial T = \Delta S_{app} \tag{A.11}$$

we can obtain the entropy ΔS_{app}. By dividing numerator and denominator of Eq. (A.11) by T

$$\partial(-\Delta G^{\circ}{}_{app}\,/\,T)\,/\,\partial T\,/\,T = \Delta S_{app} \tag{A.12}$$

and then by rearranging it, we obtain

$$\partial(-\Delta G^{\circ}{}_{app}\,/\,T)\,/\,\partial(\ln T) = \Delta S_{app} \tag{A.13}$$

Then, after the substitution of Eq. (1) in Eq. (A.13) we can calculate the derivative

$$\partial(R\ln K_{app})\,/\,\partial\ln T = \Delta S_{app} \tag{A.14}$$

and then by the equation

$$R\ln K_{app} = R\ln K_{(0)} - \xi_w R\ln\left[(W_{\mathrm{III}})_T\right] \tag{A.15}$$

we obtain

$$\partial(R\ln K_{app})\,/\,\partial\ln T = \partial\left(R\ln K_{(0)}\right)/\,\partial\ln T - \xi_w\partial(R\ln\left[(W_{\mathrm{III}})_T\right]/\,\partial\ln T. \tag{A.16}$$

This expression, by recalling Eqs. (A.11) and (12), can be rewritten, again for Class A, as

$$\Delta S_{app} = \Delta S_{Work} + \xi_w\Delta S_{Th} \tag{A.17}$$

with

$$\xi_w\Delta S_{Th} = -\xi_w R\Delta\ln\left[(W_{\mathrm{III}})_T\right] \tag{A.18}$$

Eq. (A.18), by recalling the *TED* principle of Eq. (A.6), can be rewritten as an integral

$$-\xi_w R\ln\left[(W_{\mathrm{III}})_T\right]/\left[W_{\mathrm{III}}\right] = \int_{\ln T=0}^{\ln T}\xi_w C_{p,w}\mathrm{d}\ln T = \xi_w C_{p,w}\ln T \tag{A.19}$$

that represent the thermal entropy of Eq. (5).The entropy of Eq. (A.17) is, therefore, represented by a straight line

$$\Delta S_{app} = \Delta S_{Work} + \xi_w C_{p,w}\ln T \tag{A.20}$$

with slope $\Delta C_p = \xi_w C_{p,w}$ that is exactly equal to Eq. (7) obtained from the experimental enthalpy.

Appendix B. Thermal equivalent dilution

To illustrate the principle of *thermal equivalent dilution* (*TED*), we refer to a solution of non-reacting molecules A in a solvent. If we put a dilute solution of A in contact with a concentrated solution of the same substance, we observe a spontaneous migration of solute from the concentrated to the dilute solution, so to reach the maximum dispersion of the molecules A. The maximum dispersion corresponds to the uniform mean occupation of the imaginary cells composing the solvent. The maximum dispersion is the most probable situation and corresponds to the maximum dilution compatible with the thermodynamic constraints.

There is a connection between dilution, probability and entropy. The entropy, S is related to probability P by the well known Boltzmann equation, written on a molar scale (R is the molar gas constant)

$$dS = R\mathrm{dln}P \tag{B.1}$$

It is important to point out that a diluted solute has many more possibilities (probabilities) than a concentrated one of finding a localisation cell in the solvent. Therefore, dilution is synonym of probability and hence the entropy of a diluted solution is higher than that of a concentrated solution. The relation between dilution and entropy is expressed by the relation

$$dS = R\mathrm{dln}d_{\mathrm{A}} = -R\mathrm{dln}\left[(\mathrm{A})_T\right] \tag{B.2}$$

where $[(\mathrm{A})_T]$ is the activity of the species A and [A] is its concentration. Eq. (B.1) compared with Eq. (B.2) indicates parallelism between probability and dilution and connects the experimental determination of concentration to the probability of the state and to the corresponding variation of the thermodynamic function entropy, S.

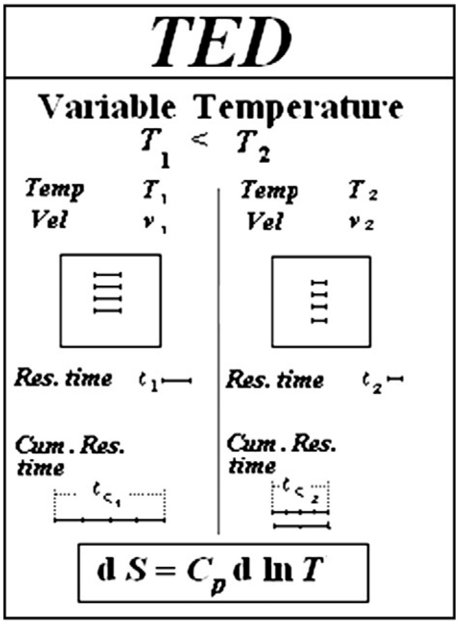

Fig. B.1. Thermal Equivalent Dilution: temperature, cumulative residence time, t_c and entropy. t_c is like a virtual concentration.

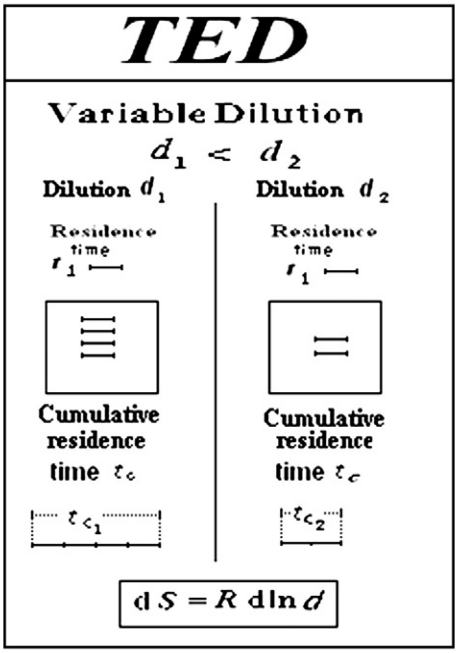

Fig. B.2. Thermal Equivalent Dilution: dilution, cumulative residence time and entropy. The cumulative residence time t_c is like a real concentration.

For the relation between entropy and temperature, we observe that the non-reacting solute A is composed of particles that are moving in complete disorder, exchanging continuously one another their thermal energy. We imagine to look at the solution by a hypothetical molecular microscope and we open in the viewer a window for a fixed time unit, then we register photographically the trajectories of all the particles passing through the window (Fig. B.1). If we measure the length of each trace, l, and calculate its reciprocal we obtain the residence time $t_{res} = 1/l$, that is the time needed to cover by the molecule the length unit. If we sum up the times t_{res} of all the particles, we can measure the cumulative residence time $t_{c,1}$ that indicates how long time the particles altogether have resided in the window. If we repeat the experiment at a higher temperature T_2 whereby the particles increase their velocity, we observe that the cumulative residence time $t_{c,2}$ is shorter. The dispersion of the particles is proportional to $C_{p,A}$, the isobaric heat capacity of molecule A, and hence the entropy of the units is increased by the temperature change according to

$$dS = C_{p,A}\mathrm{dln}T \tag{B.3}$$

and it is clear that the cumulative residence time t_c is inversely proportional to $\ln T$ and can be considered as virtual concentration. The analogy of Eq. (B.2) with Eq. (B.3) suggests an analogy between dilution and temperature effects. In fact, we can demonstrate that the cumulative residence time of the solute undergoes a parallel change with temperature and with dilution. If we repeat the experiment of the window in the microscope at constant temperature but variable dilution (Fig. B.2), we observe that by increasing the dilution we make the total residence time decreasing as by increasing the temperature and in correspondence we observe that the entropy is increasing according to Eq. (B.2). The two effects of temperature and dilution can be combined. If we set for the species A the activity $[(\mathrm{A})_T] = f_{\mathrm{A}}\cdot [\mathrm{A}]$, where [A] is the concentration and $f_{\mathrm{A}}\cdot$ is the activity coefficient, then $d_{\mathrm{A}} = 1/[(\mathrm{A})_T]$ is the dilution and $1/f_{\mathrm{A}}$ is the *thermal equivalent dilution* coefficient. We can calculate

$$\mathrm{d}S_{\mathrm{A}} = -R\mathrm{dln}\left[(A)_T\right] = -R\mathrm{dln}[\mathrm{A}] - R\mathrm{dln}f_{\mathrm{A}} \tag{B.4}$$

On the other hand, the total differential of entropy is

$$\mathrm{d}S_{\mathrm{A}} = \left(\partial S_{\mathrm{A}} / \partial\ln\left[(\mathrm{A})_T\right]\right)_T \mathrm{dln}[\mathrm{A}] + \left(\partial S_{\mathrm{A}} / \partial\ln T\right)_{[\mathrm{A}]}\mathrm{dln}T = -R\mathrm{dln}[\mathrm{A}] + C_{p,A}\mathrm{dln}T \tag{B.5}$$

By comparison of Eq. (B.4) with Eq. (B.5) we have the equality

$$-Rd\ln f_A = C_{p,A}d\ln T \tag{B.6}$$

and then, being, at constant [A], $\mathrm{dln}[(\mathrm{A})_T] = \mathrm{dln}\, f_{\mathrm{A}}$ we obtain

$$-\partial\ln\left[(\mathrm{A})_T\right] / \partial\ln T = C_{p,A} / R \tag{B.7}$$

that we call *thermal equivalent dilution* (*TED*) [25] principle. If we refer to ξ_w stoichiometric units, we obtain

$$-\xi_w R d \ln\left[(A)_T\right] = \xi_w C_{p,A} d \ln T \tag{B.8}$$

The integral of the r.h.s. of Eq. (B.8) between the limits ln*T* (upper limit, molecule in thermal agitation) and ln*T* = 0 (lower limit, molecule at rest) represents the thermal entropy of Eq. (5).

Use of *TED* has been done to determine the stoichiometric coefficient ξ_w in every hydrophobic process, as shown in Appendix A.

The applicability of *TED* principle to the hydrophobic hydration processes in aqueous solutions at different temperatures represents an experimental proof of the "Ergodic Hypothesis". The ergodic hypothesis in statistical analysis assumes that the average of a process parameter over time and the average over the statistical ensemble are the same, just the assumption on which *TED* is based if we consider the temperature a time variable, determining the velocity of the molecules. The fact that, by mean of *TED* so many coherent responses are obtained, can be considered as a valid proof that the ergodic hypothesis is working. Hence, it is no more a hypothesis, rather we can speak of an "Ergodic Property".

Appendix C. Analysis of non-thermal extrapolated thermodynamic functions

The analysis and consequent disaggregation of the extrapolated values *i.e.* the intercepts, ΔH_{Work} of Eq. (3) and ΔS_{Work} of Eq. (4) for Class A and Class B, give further support to the idea of the real meaning of ξ_w, as related to the number of water molecules W_{III} and to the volume of the cavity. All these extrapolated values are thermodynamic functions devoid of thermal energy, *i.e.* extrapolated to $T = 0$ for enthalpy or to ln*T* = 0, for entropy.

If we plot the values of ΔH_{Work} for one homogenous series of processes of Class A against the number ξ_w of each element of the series we obtain exact linear plots

$$\Delta H_{Work} = \Delta H_0^{(\xi_w = 0)} + \xi_w \Delta h_{for} \tag{C.1}$$

The coefficients of the equations found for each series are reported in Table C.1.

We observe that the values of the coefficients Δh_{for} in the different series show a very narrow variability and justify the calculation of a mean, by assuming that in every series we are dealing with the same molecular process.

Analogously, if we plot the values of ΔS_{Work} (*i.e.* non-thermal extrapolated to ln*T* = 0) for one homogeneous series of processes of Class A against the respective number ξ_w, we obtain a nice linear plot

$$\Delta S_{Work} = \Delta S_0^{(\xi_w = 0)} + \xi_w \Delta s_{for} \tag{C.2}$$

As example of these plots, we report the diagram for gases (Fig. C.1). The coefficients of the equations for the extrapolated entropy of Class A are reported in Table C.2.

Table C.1
Class A. Equations found for extrapolated enthalpy.

Process	$\Delta H_0^{(\xi w = 0)}$	ξ_w Δh_{for}	Unit	ξ_w range
Gas dissolut.	−17.7	$-21.6 \cdot \xi_w$	kJ mol^{-1}	2–6
Liquid dissol.	+4.6	$-23.3 \cdot \xi_w$	kJ mol^{-1}	2.7–5.4
Protein denat.	+211.8	$-22.1 \cdot \xi_w$	kJ mol^{-1}	80–140
Proton. carboxyl.	+0.1	$-21.8 \cdot \xi_w$	kJ mol^{-1}	1.8–2.3

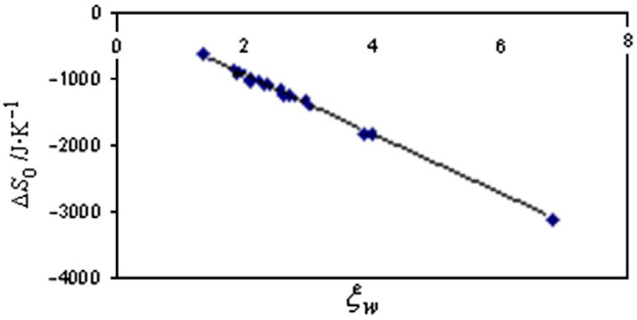

Fig. C.1. Class A. Gases. Extrapolated entropy ΔS_{Work} against the number ξ_w.

The same comments as done for the coefficients of enthalpy, hold for those of entropy and confirm that all these reactions form a homogeneous group based on the same molecular reaction.

An equation similar to Eq. (C.1) is found if we plot the extrapolated enthalpy ΔH_{Work} of processes of Class B against the respective value of ξ_w. The coefficients of the equation for enthalpy in Class B are reported in Table C.3.

Although the number of series examined is not large enough to give significant means we can observe that the results are not against the hypothesis of a common group.

Again, we find an equation similar to Eq. (C.2) when we plot the values of the extrapolated entropy of Class B. The coefficients of the equations are reported in Table C.4. For these coefficients of entropy again we find values that are not in contradiction with the existence of a common reaction. Moreover if we compare the mean values of the coefficients for enthalpy and entropy of Class B with the corresponding mean values in Class A we observe that the numerical values are very close to one another but the signs are opposite. This finding confirms not only that in each Class we are dealing with the same reaction but that in the two Classes we are finding the same reaction in opposite direction. The intercepts ΔH_{Work} and ΔS_{Work} of Class A and Class B are, therefore, functions of the respective number ξ_w. The thermal components ΔH_{Th} and ΔS_{Th}, however, are functions of these numbers and therefore we can express the apparent enthalpy

Table C.2
Class A. Equations found for extrapolated entropy.

Procass	$\Delta S_0^{(\xi_w = 0)}$	ξ_w Δs_{for}	Unit	ξ_w range
Gas dissolut.	−86.4	$-445.4 \cdot \xi_w \pm 7$	J K^{-1} mol^{-1}	2–6
Gas (Privalov)	−78.5 ± 23	$-450 \cdot \xi_w$	J K^{-1} mol^{-1}	
Ebull. (Trouton)	−86.9 ± 1.4		J K^{-1} mol^{-1}	
Liquid dissol.	−0.5	$-447 \cdot \xi_w$	J K^{-1} mol^{-1}	2.7 –5.4
Protein denat.	+415	$-428.5 \cdot \xi_w$	J K^{-1} mol^{-1}	80–140
Proton. acids[a]	+104	$-442.6 \cdot \xi_w$	J K^{-1} mol^{-1}	1.8–2.3
Cycl. peptides	+16	$-446 \cdot \xi_w$	J K^{-1} mol^{-1}	

[a] These values refer to K_{for} in Eq. (25).

Table C.3
Class B. Equations found for extrapolated enthalpy.

Process	$\Delta H_0^{(\xi_w = 0)}$	ξ_w Δh_{red}	Unit	Range of ξ_w
Micelle	−4.22	$+23.2 \cdot \xi_w$	kJ mol^{-1}	4–19
Bio-complx	−120.9	$+24.3 \cdot \xi_w$	kJ mol^{-1}	19–189

Table C.4
Class B. Equations found for extrapolated entropy.

Process	$\Delta S_0^{(\xi_w = 0)}$	ξ_w Δs_{red}	Unit	ξ_w range
Micelle	+10.2	$+428 \cdot \xi_w \pm 33$	J K^{-1} mol^{-1}	4–19
Bio-complx	+262	$+436.2 \cdot \xi_w$	J K^{-1} mol^{-1}	19–189

and apparent entropy in a homogeneous scheme of equations, each of which is composed of three terms:

1) Class A, Enthalpy

$$\Delta H_{app} = \Delta H_0^{(\xi_w=0)} + \xi_w \Delta h_{for} + \xi_w C_{p,w} T \tag{C.3}$$

2) Class A, Entropy

$$\Delta S_{app} = \Delta S_0^{(\xi_w=0)} + \xi_w \Delta s_{for} + \xi_w C_{p,w} \ln T \tag{C.4}$$

3) Class B, Enthalpy

$$\Delta H_{app} = \Delta H_0^{(\xi_w=0)} + \xi_w \Delta h_{red} - \xi_w C_{p,w} T \tag{C.5}$$

4) Class B, Entropy

$$\Delta S_{app} = \Delta S_0^{(\xi_w=0)} + \xi_w \Delta s_{red} - \xi_w C_{p,w} \ln T \tag{C.6}$$

In each equation from Eqs. (C.3) to (C.6), the sum of the first and second terms of the r.h.s. constitutes the work components ΔH_{Work} or ΔS_{Work}. The third terms of the r.h.s. of these equations represent the thermal components ΔH_{Th} or ΔS_{Th}. We note that Eqs. (C.5) and (C.6) for Class B contain the thermal components ΔH_{Th} and ΔS_{Th} with minus sign due to the *association* process of $-\xi_w$ water molecules W_{III}, whereas Eqs. (C.3) and (C.4) for Class A have the thermal components with plus sign due to the *dissociation* process of $+\xi_w$ water molecules W_{III}.

An interesting point to clarify is that the thermal components ΔH_{Th} and $-T\Delta S_{Th}$ compensate each other and do not contribute to free energy ($\Delta G_{Th} = 0$). In fact, we calculate for each class

$$\begin{aligned}\Delta G_{Th} &= \Delta H_{Th} - T\Delta S_{Th} = 0 + \int_0^T \Delta C_p \mathrm{d}T - 0 - T\int_0^T \Delta C_p \mathrm{d}\ln T \\ &= 0 + \int_0^T \Delta C_p \mathrm{d}T - 0 - \int_0^T \Delta C_p \mathrm{d}T = 0\end{aligned} \tag{C.7}$$

and this is valid whatever is the upper temperature. The thermal components, ΔH_{Th} and ΔS_{Th}, however, affect significantly the dependence of ΔG_{app} upon the temperature, because as shown in equations from Eqs. (C.3) to (C.6) they sum up with ΔH_{Work} and ΔS_{Work}, respectively, to give ΔH_{app} and ΔS_{app}. The latter quantities are those that generate the curvature of the van't Hoff plot.

References

[1] E. Fisicaro, C. Compari, E. Duce, A. Braibanti, Entropy changes in aqueous solutions of non-polar substances, J. Solution Chem. 37 (2008) 487–501.

[2] E. Fisicaro, C. Compari, A. Braibanti, Entropy/enthalpy compensation: hydrophobic effect, micelles and protein complexes, Phys. Chem. Chem. Phys. 6 (2004) 4156–4166.

[3] E. Fisicaro, C. Compari, A. Braibanti, Response to comment on "Entropy/enthalpy compensation: hydrophobic effect, micelles and protein complexes, Phys. Chem. Chem. Phys. 7 (2005) 1324–1325.

[4] E. Fisicaro, C. Compari, E. Duce, M. Biemmi, M. Peroni, A. Braibanti, Thermodynamic of micelle formation in water, hydrophobic processes and surfactant self-assemblies, Phys. Chem. Chem. Phys. 10 (2008) 1–12.

[5] W. Kauzmann, Some factors in the interpretation of protein denaturation, Adv. Protein Chem. 14 (1959) 1–63.

[6] L.R. Pratt, D. Chandler, Theory of the hydrophobic effect, J. Chem. Phys. 67 (1977) 3683–3704.

[7] C. Tanford, The Hydrophobic Effect: Formation of Micelles and Biological Membranes, Wiley, New York, 1973.

[8] C. Tanford, Contribution of hydrophobic interactions to the stability of the globular conformation of proteins, J. Am. Chem. Soc. 84 (1962) 4240–4247.

[9] A. Ben-Naim, Solvation Thermodynamics, Plenum, New York, 1987.

[10] I.M. Klotz, Non-covalent bonds in protein structure, Brookhaven Symp. Biol. 13 (1960) 25–48.

[11] B. Guillot, Y. Giussani, A computer simulation study of the temperature dependence of the hydrophobic hydration, J. Chem. Phys. 99 (1993) 8075–8094.

[12] B. Lee, G. Graziano, A two-state model of hydrophobic hydration that produces compensating enthalpy and entropy changes, J. Am. Chem. Soc. 118 (1996) 5163–5168.

[13] G. Graziano, A van der Waals approach to the entropy convergence phenomenon, Phys. Chem. Chem. Phys. 6 (2004) 406–410.

[14] W. Pfeil, P.L. Privalov, Thermodynamic investigations of proteins. I. Standard functions for proteins with lysozyme as an example, Biophys. Chem. 4 (1976) 23–32.

[15] P.L. Privalov, Thermodynamic investigations of biological macromolecules, Pure Appl. Chem. 47 (1976) 293–304.

[16] P.L. Privalov, S.J. Gill, Stability of protein structure and hydrophobic interaction, Adv. Protein Chem. 39 (1988) 191–234.

[17] P.L. Privalov, Thermodynamic problems of protein structure, Ann. Rev. Biophys. Biophys. Chem. 18 (1989) 47–69.

[18] P.L. Privalov, Thermal investigations of biopolymer solutions and scanning microcalorimetry, FEBS Letts. 40 (1974) S140–S153.

[19] J.M. Sturtevant, Applications of calorimetry in biochemistry and biology, Adv. Biophys. Bioeng. 3 (1974) 35–51.

[20] J.M. Sturtevant, Biochemical applications of differential scanning calorimetry, Ann. Rev. Phys. Chem. 38 (1987) 463–468.

[21] J.F. Brandts, L. Hunt, The thermodynamics of protein denaturation. 3. The denaturation of ribonuclease in water and in aqueous urea and aqueous ethanol mixtures, J. Am. Chem. Soc. 89 (1967) 4826–4838.

[22] R. Lumry, Uses of enthalpy–entropy compensation in protein research, Biophys. Chem. 105 (2003) 545–557.

[23] R. Lumry, in: A. Braibanti (Ed.), Bioenergetics and Thermodynamics: Model Systems, Interpretation of Calorimetric Data from Cooperative Systems, Reidel, Dordrecht, 1980, p. 405;
D.F. Shiao, R. Lumry, J. Fahey, Chymotrypsinogen family of proteins. XI. Heat-capacity changes accompanying reversible thermal unfolding of proteins, J. Am. Chem. Soc. 93 (1971) 2024–2035.

[24] D.J. Winzor, C.M. Jackson, Interpretation of the temperature dependence of equilibrium and rate constants, J. Mol. Recognit. 19 (2006) 389–407.

[25] A. Braibanti, E. Fisicaro, C. Compari, Thermal equivalent dilution, J. Phys. Chem. B 102 (1998) 8537–8539.

[26] D.T. Haynie, Biological Thermodynamics, Cambridge Univ. Press, Cambridge, 2001.

[27] D.P. Kharakoz, Partial molar volumes of molecules of arbitrary shape and the effect of hydrogen bonding with water, J. Solution Chem. 21 (1992) 569–595.

[28] D.P. Kharakoz, Volumetric properties of proteins and their analogs in diluted water solutions. 1. Partial volumes of amino acids at 15–55 degrees C, Biophys. Chem. 34 (1989) 115–125.

[29] E. Wilhelm, R. Battino, R.J. Wilcock, Low-pressure solubility of gases in liquid water, Chem. Rev. 77 (1977) 219–262.

[30] A. Braibanti, E. Fisicaro, F. Dallavalle, J.D. Lamb, J.L. Oscarson, Probability, thermodynamics and dispersion space for a statistical model of equilibria in solution. 2. Concentration and temperature moments of partition function, J. Phys. Chem. 97 (1993) 8062–8070.

[31] P.W. Atkins, Elem. of Physical Chemistry, Oxford Press, Oxford, 1992, p. 90.

[32] A. Braibanti, E. Fisicaro, A. Ghiozzi, C. Compari, M. Panelli, Solubility of inert gases and liquid hydrocarbons in water, J. Solution Chem. 24 (1995) 703–718.

[33] A. Ben-Naim, J. Wilf, H. Yaacobi, Hydrophobic interaction in light and heavy water, J. Phys. Chem. 77 (1973) 95–102.

[34] S.J. Gill, N.F. Nichols, I. Wadsö, Calorimetric determination of enthalpies of solution of slightly soluble liquids. I. Application to benzene in water, J. Chem. Thermodyn. 7 (1975) 175–183.

[35] A. Braibanti, E. Fisicaro, F. Dallavalle, J.D. Lamb, J.L. Oscarson, F.X. Ughi, Probability, thermodynamics, and dispersion space for a statistical model of equilibria in solution. 3. Aqueous solutions of monocarboxylic acids at different temperatures, J. Phys. Chem. 97 (1993) 8071–8081.

[36] A. De Robertis, C. De Stefano, C. Rigano, S. Sammartano, Thermodynamic parameters for the protonation of carboxylic acids in aqueous tetraethylammonium iodide solutions, J. Solution Chem. 19 (1990) 569–587.

[37] D.D.J. Wright, The dissociation constant of chloroacetic acid from 0 °C to 40 °C, J. Am. Chem. Soc. 56 (1934) 314–317.

[38] F.S. Feates, D.J.G. Ives, Ionization functions of cyanoacetic acid in relation to the structure of H_2O and the hydration of ions and molecules, J. Chem. Soc. (1956) 2798–2812.

[39] H.S. Harned, R.W. Ehlers, The dissociation constant of acetic acid from 0 °C to 60 °C, J. Am. Chem. Soc. 55 (1933) 652–656.

[40] J.C. Lee, S.N. Timasheff, In vitro reconstitution of calf brain microtubules: effects of solution variables, Biochemistry 16 (1979) 1754–1764.

[41] H.J. Hinz, M.J. Gorbunoff, B. Price, S.N. Timasheff, Heat capacity microcalorimetry of the in-vivo reconstitution of calf brain microtubules, Biochemistry 18 (1979) 3084–3089.

[42] J.-H. Ha, R.S. Spolar, M.T. Jr Record, Role of the hydrophobic effect in stability of the site-specific protein–DNA complexes, J. Mol. Biol. 209 (1989) 801–816.

[43] S. Cabani, P. Gianni, V. Mollica, L. Lepori, Group contributions to the thermodynamic properties of nonionic organic solutes in dilute aqueous solution, J. Solution Chem. 10 (8) (1981) 563–595.

[44] S. Cabani, Thermodynamic properties of polar and non-polar solutes in aqueous solution, Port, Electrochim. Acta 3 (1985) 5–20.

[45] D. Chandler, Two faces of water, Nature 417 (2002) 491.

[46] D. Chandler, Insight Review: interfaces and the driving force of hydrophobic assembly, Nature 437 (2005) 640–647.

[47] G. Nemethy, H.A. Scheraga, Structure of water and hydrophobic bonding in proteins. I. A model for the thermodynamic properties of liquid water, J. Chem. Phys. 36 (1962) 3382–3400.

[48] B. Widom, P. Bhimalapuram, K. Koga, The hydrophobic effect, Phys. Chem. Chem. Phys. 3 (2003) 3085–3093.

[49] K.A. Sharp, B. Madam, Hydrophobic effect, water structure, and heat capacity changes, J. Phys. Chem. 101 (1997) 4343–4348.

[50] F. Vanzi, B. Madam, K.A. Sharp, Effect of the protein denaturants urea and guanidinium on water structure: a structural and thermodynamic study, J. Am. Chem. Soc. 120 (1997) 10748–10753.
[51] A. Pohorille, L.R. Pratt, Cavities in molecular liquids and the theory of hydrophobic solubilities, J. Am. Chem. Soc. 117 (1998) 5066–5074.

Glossary

W_I: water in clusters composed of m molecules, $(\mathrm{W}_m)_{\mathrm{I}}$,
W_{II}: water in short chains composed of $(m-1)$ molecules, $(\mathrm{W}_{m-1})_{\mathrm{II}}$
W_{III}: free water molecules
TED: Thermal Equivalent Dilution (based on Ergodic Hypothesis)
Class A: Hydroph. Hydr. Proc. with reaction A$(-\xi_w\mathrm{W}_{\mathrm{I}} \rightarrow \xi_w\mathrm{W}_{\mathrm{II}} + \xi_w\mathrm{W}_{\mathrm{III}} + \text{cavity})$
Class B: Hydroph. Hydr. Proc. with reaction B$(-\xi_w\mathrm{W}_{\mathrm{II}} - \xi_w\mathrm{W}_{\mathrm{III}} \rightarrow \xi_w\mathrm{W}_{\mathrm{I}} - \text{cavity})$
ξ_w: $|n_w|$ stoichiometric coefficient of $\mathrm{W}_{\mathrm{III}}$, determined by *TED*
$(-\Delta G^{\o}_{app})/RT$: $\ln K_{app} = f(1/T)$, plot, with min. in Class A, with max. in Class B
K_{app}: $k_{sol} = x_2$ (molar fraction) in dissolution of gases or liquids
id.: K_{den} in denaturation
id.: $K_{mic} = 1/cmc$ in micelle formation
id.: K_H in protonation of carboxylic acids
id.: K_f in bio-complexation
ΔH_{app}: enthalpy obtained as tangent of $\ln K_{app} = f(1/T)$ or by calorimetry
ΔC_p: $+\xi_w\, C_{p,w}$: (Class A), slope both in $\Delta H_{app} = f(T)$ and in $\Delta S_{app} = f(\ln T)$
id.: $-\xi_w\, C_{p,w}$: (Class B), slope both in $\Delta H_{app} = f(T)$ and in $\Delta S_{app} = f(\ln T)$
$C_{p,w}$: isobaric heat capacity of liquid water $= 75.36\ \mathrm{J\,K^{-1}\,mol^{-1}}$
ΔS_{app}: entropy obtained by Helmholtz-Gibbs equation
$[(W_{III})_T]$: activity of the species $\mathrm{W}_{\mathrm{III}}$, temperature dependent
$1/[(W_{III})_T]$: dilution of species $\mathrm{W}_{\mathrm{III}}$, temperature dependent
n_w: stoichiom. coeff. of species $\mathrm{W}_{\mathrm{III}}$, from ΔC_p
$+\xi_w$: n_w in Class A
$-\xi_w$: n_w in Class B
$-n_w \partial \ln[(W_{III})_T]/\partial \ln T$: changing of K_{app} with temperature (by *TED*)
V_2: $19.9\ \mathrm{cm^3\,mol^{-1}}\,\xi_w^{-1}$, partial volume of liquid water
ΔV: volume change for cavity formation
$-\Delta V$: volume change for cavity reduction
$\Delta H_0^{(\xi_w=0)}$: non-thermal enthalpy, extrapolated to $\xi_w = 0$, indep. from temperature and cavity
$\Delta S_0^{(\xi_w=0)}$: non-thermal entropy, extrapolated to $\xi_w = 0$, indep. from temperature and cavity
$\Delta S_{condens}$: entropy change for vapour condensation (Trouton law)
$\Delta H_{for} < 0$: enthalpy change for cavity formation, Class A
$\Delta h_{for} < 0$: unitary $(\xi_w = 1)$ enthalpy change for cavity formation, Class A
$<\Delta h_{for}> < 0$: mean unitary enthalpy change in Class A
$\Delta S_{for} < 0$: entropy change for cavity formation, Class A
$\Delta s_{for} < 0$: unitary $(\xi_w = 1)$ entropy change for cavity formation, Class A
$<\Delta s_{for}> < 0$: mean unitary entropy change for cavity formation in Class A
$\Delta H_{red} > 0$: enthalpy change for cavity reduction, Class B
$\Delta h_{red} > 0$: unitary $(\xi_w = 1)$ enthalpy change for cavity reduction, Class B
$<\Delta h_{red}> > 0$: mean unitary enthalpy change for cavity reduction in Class B
$\Delta S_{red} > 0$: entropy change for cavity reduction, Class B
$\Delta s_{red} > 0$: unitary $(\xi_w = 1)$ entropy change for cavity reduction, Class B
$<\Delta s_{red}> > 0$: mean unitary entropy change for cavity reduction in Class B
$\Delta H_{Th} > 0$: $\xi_w C_{p,w}\, T$, thermal enthalpy, Class A
$\Delta H_{Th} < 0$: $-\xi_w C_{p,w}\, T$, thermal enthalpy, Class B
$\Delta S_{Th} > 0$: $\xi_w C_{p,w} \ln T$, thermal entropy, Class A
$\Delta S_{Th} < 0$: $-\xi_w C_{p,w} \ln T$, thermal entropy, Class B
$\Delta G_{Th} = 0$: from $\Delta H_{Th} - T\Delta S_{Th} = 0$, in both Classes A and B
ΔH_{Work}: non-thermal work enthalpy, in both Classes A and B, extrapol. to $T = 0$
ΔS_{Work}: non-thermal work entropy, in both Classes A and B, extrapol. to $\ln T = 0$
ΔG_{Work}: work free energy (non-thermal)
$\log K_{calc}$: $(-\Delta G_{calc}/2.302RT)$ from $\Delta H_{for}$and ΔS_{for} in carboxylic acids
$\Delta \log K_x$: $\log K_{app} - \log K_{calc}$ (in carboxylic acids)
$\Delta \log K_x$: $= \log K_{prot}$ (in carboxylic acids)
$\Delta \xi_w$: change in ξ_w due to substituent effect on ΔC_p